Chapter VIII

The cell cycle

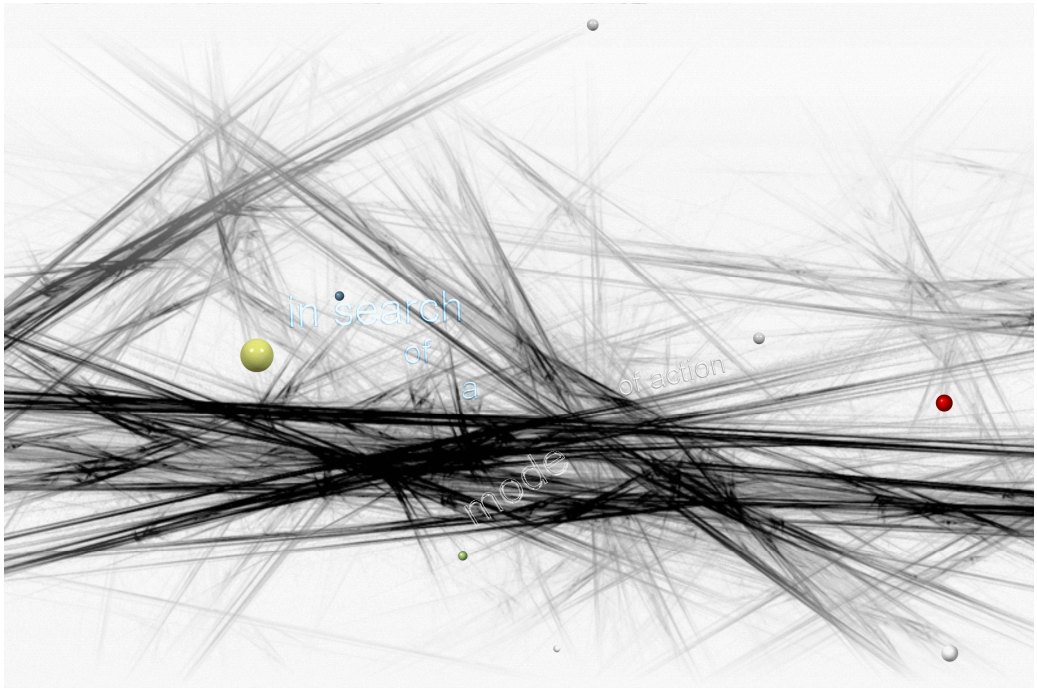

8.1 Introduction

Cell cycle is arguably the most fundamental process that occurs in eukaryotic cells and is quite literally a matter of life and death (Thomas and Goodyer, 2003). The stages vary greatly in duration among cell types, but typical time spans are as follows (Hernandez and Rathinavelu, 2006):

- *S* phase: 10 to 20 hours. This is the synthesis phase, where DNA replication occurs.
- *M* phase: 0.5 to 1 hour. This phase is where mitosis occurs; mitosis is the actual cell division where the two DNA copies separate.
- G_1 and G_2 phases: The duration of the G_2 phase is in the same range of 2 to 10 hours. These are gaps that occur between mitosis and synthesis, which prepare the cell for the next phase.
- G_0 phase: A sub-phase of G_1 in which the cells are resting, i.e., they are not preparing to divide.

The DNA content of cell nuclei varies through the cell cycle in a predictable fashion- cells in G_2 or M have twice the DNA content of cells in G_1, and cells undergoing DNA synthesis in *S* phase have an intermediate amount of DNA (Thomas and Goodyer, 2003).

8.1.1 Cell cycle regulation

The progression of the cell cycle is tightly regulated by defined temporal and spatial expression, localisation and destruction of several cell cycle regulators, which exhibit highly dynamic behaviour during the cell cycle (Thomas and Goodyer, 2003). It is firmly established that a family of protein kinases, termed cyclin-dependent kinases (CDKs), controls the transitions between successive phases of the cell cycle in all eukaryotic cells (Nigg, 1995). CDKs are serine/threonine protein kinases that are activated at specific points of the cell cycle (Schafer, 1998). Sequential formation, activation and subsequent inactivation of cyclins and CDKs are critical for the control of the cell cycle (Kurita-Ochiai *et al.,* 2006). In addition, CDK inhibitors (CDKIs) can play a key role in

controlling cell cycle progression by negatively regulating CDK activities at specific times in the cycle.

Table 8.1. Cyclin-CDK complexes are activated at specific points of the cell cycle. CAK, CDK activating kinase (Vermeulen *et al.,* 2003).

CDK		Cyclin	Cell cycle phase activity
CDK4		Cyclin D1, D2, D3	G_1 phase
CDK6		Cyclin D1, D2, D3	G_1 phase
CDK2		Cyclin E	G_1/S phase transition
CDK2		Cyclin A	S phase
CDK1	(cdc2)	Cyclin A	G_2/M phase transition
CDK1	(cdc2)	Cyclin B	Mitosis
CDK7		Cyclin H	CAK, all cell cycle phases

There are two classes of mammalian CDKI known to date (Park *et al.,* 2002). One group is the CIP/KIP family, including p21, p27 and p57 having broad specificity. The other is the INK4 family, including p15, p16, p18 and p19, which target the CDK4 and CDK6 (*Fig. 8.1*).

In normal human cells, the diverse checkpoints represent fail-safe mechanisms whose key role is to avoid the accumulation of genetic errors during cell division (Bartek *et al.,* 1999). Among the best-known checkpoints are G_1 arrest mediated by p53/p21 axis in response to DNA damage, checkpoints that monitor the quality of DNA replication and the occurrence of DNA damage during the S-phase, and the status of spindle assembly in mitosis. Although some DNA damage checkpoint cascades respond to DNA damage in quiescent cells, most operate only in proliferating cells, with the nature of the response dependent on variables such as cell type and differentiation, extent of DNA damage, and the position of the cell in the cell cycle (Scott *et al.,* 2004). Thus normal cells that have not passed the G_1 restriction point will arrest in G_1, S-phase cells will undergo a delay in S and may undergo a subsequent G_2 arrest, and those cells already in G_2 will be prevented from entering M-phase until repair of potentially lethal damage is complete.

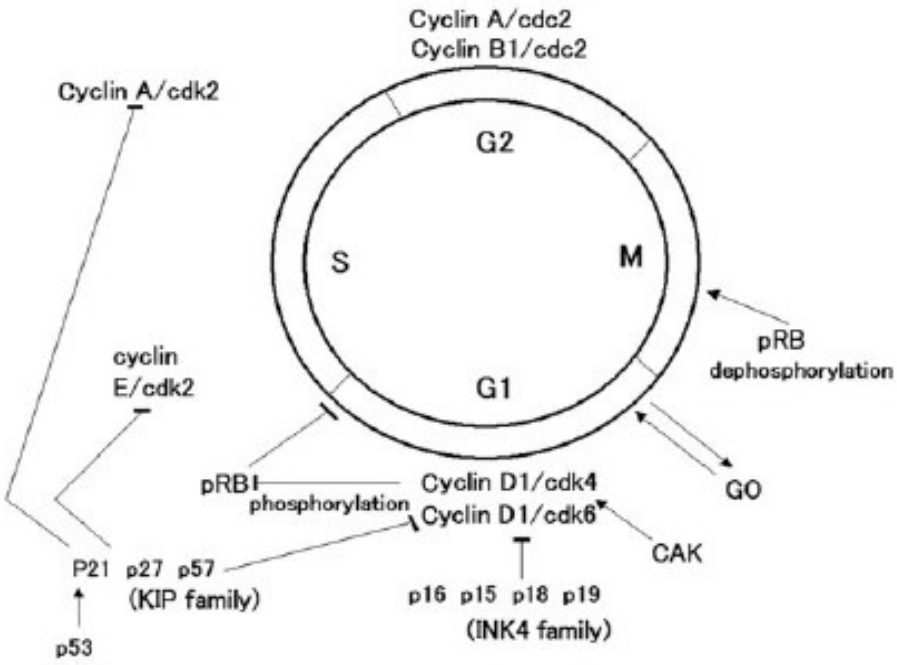

Fig. 8.1: Scheme of cell cycle regulation. CAK, cdk-activating kinase; cdk, cyclin-dependent kinase; INK4, inhibitor of cdk4; KIP, kinase inhibitor protein; pRB, retinoblastoma protein (Dobashi, 2005).

8.2 Cell cycle and carcinogenesis

The cell cycle is an ubiquitous, complex process involved in the growth and proliferation of cells, organismal development, regulation of DNA damage repair, tissue hyperplasia as a response to injury, and diseases such as cancer (Schafer, 1998). Cancer is increasingly viewed as a cell cycle disease (Bartek *et al.,* 1999). This view reflects the evidence accumulated that the vast majority of, and quite likely all tumours have suffered one or more defects that derail the cell cycle machinery. The process of tumourigenesis leads to multiple genetic changes that alter the regulation of signalling pathways, such as those involved in cell cycle and mitotic spindle checkpoints, DNA repair, and apoptosis that lead to further molecular abnormalities and increased cell proliferation (Scott *et al.,* 2004).

Most, if not all, human cancers show a deregulated control of G_1 phase progression, a period when cells decide whether to start proliferating or to stay quiescent (Golias *et al.,* 2004). In the normal cell, oncoproteins carry a signal from

the cell surface to the nucleus with the end result being transcription and initiation of the cell cycle (Schafer, 1998). In transformed cells these signal transduction pathways are always "turned on" or their inhibitory pathways are "turned off" (*Table 8.2*).

Table 8.2. Cell cycle regulators in neoplasia

Oncoprotein/ Tumour suppressor	**Normal cell cycle function**	**Oncogenic alteration**
p53	Promotes G_1 arrest after DNA damage	Mutation
pRb	Restriction point regulator	Deletion
Mdm-2	Overrides p53 transcriptional activity	Gene amplification or enhanced mRNA translation
P16	Inactivates G_1 cyclin-cdk complexes	Deletion
Cyclin D1	Initiates cell cycle	Gene amplification
Cdc25A, cdc25B	Activates G_1/S cdks	Overexpression

In terms of molecular pathogenesis of cancer, cell cycle defects can either represent the initial, predisposing event, or contribute to tumour progression (Bartek *et al.,* 1999). The tumour suppressor gene p53 codes for a transcription factor which regulates oncogene expression, gene transcription, and DNA synthesis and repair systems, as well as apoptosis (Ahn *et al.,* 2002). As a transcription factor, the p53 protein binds to a specific sequence on the promoter region and then activates the transcription of cellular genes. In normal cells, DNA damage induces p53 expression, leading to cell cycle arrest in the G_1 phase and apoptosis, as well as inhibition of DNA replication. However, normal function of p53 is missing in immortalised cells. It has been reported that, except for cervical cancers, most (50%) cancer development results from p53 gene mutation.

8.3 Cell cycle and chemotherapy

The prediction of tumour behaviour and response to treatment has led to interest in the assessment of the proliferative potential of tumours (Golias *et al.,* 2004). Understanding the molecular details of the cell cycle regulation and checkpoint abnormalities in cancer, and manipulation of these control mechanisms offers

insight into potential therapeutic strategies. Anti-cancer agents may alter one or more regulatory events in the cell cycle resulting in blockade of cell cycle progression, thereby reducing the growth and proliferation of the cancer cells (Adhami *et al.,* 2004). For example, the function of p53 in sentencing inappropriately growing cells to death has implications for cancer development and chemotherapy (Collins *et al.,* 1997). Murine tumours with functional p53 respond to chemotherapy by promoting their own demise, but those lacking p53 typically do not.

Initially, some anti-cancer agents were investigated for their abilities to inhibit cell cycle transitions and suppress hyperproliferation by either down-regulating cyclin/cdk expression or up-regulating the CKI (Dobashi, 2005). Now, however, much attention is being paid to their potential for inducing apoptosis. The up-to-date rational drug development in cancer therapy appears to concentrate on the discovery of effective pharmaceutical reagents that can intervene diverse signaling pathways (Liu *et al.,* 2005). The regulatory system that controls normal cell proliferation and cell death stays balanced through orchestrated cascades of multiple interacting signalling routes. When this rhythmic scheme is perturbed by biochemical agents, it often results in the breakdown of cell cycle machinery, subsequently entering into apoptosis.

The most potent anti-cancer drugs act by damaging DNA; their effect is greatest during the S phase (Hernandez and Rathinavelu, 2006). Other anti-cancer drugs, such as Taxol™ block the formation of the mitotic spindle in the M phase. For anti-cancer drugs to be effective, a high percentage of tumour cells must be undergoing division (S and M phases). Anti-folates such as methotrexate, trimetrexate and CB3717 (N^{10}-propargyl-5,8-dideazafolic acid) tend to cause accumulation of cells in S phase or at the G_1/S interphase (Skelton *et al.,* 1999). Agents which disrupt formation of the mitotic spindle, such as the *Vinca* alkaloids, arrest cells in G_2/M, phase.

Replication process is directly disrupted with DNA-damaging agents such as cisplatin, mitomycins, bleomycins, etoposide and irinotecan (a camptothecin derivative) (Owa *et al.,* 2001). Camptothecin (CPT) is a DNA topoisomerase I

inhibitor that blocks the DNA religation of topoisomerase I cleavage complexes (Zhou *et al.,* 2002). During DNA replication, the collision between topoisomerase I cleavage complexes and DNA replication forks generates double-strand breaks. Therefore, CPT is most potent during DNA replication and arrest of cells in G_2 phase results in DNA damage. CPT derivatives are used clinically to treat many types of solid tumours, including colorectal and ovarian carcinomas, but not all cancer cell lines are equally sensitive to it.

8.4 Determination of the effect of Pg 8 and [Au(dppe)$_2$]Cl on cell cycle of Jurkat cells

It has been shown (**Chapter 7**) that **Pg 8** and [Au(dppe)$_2$]Cl caused Jurkat cells to undergo apoptosis after exposure for 48 h. The aim of this experiment was to determine if cell death was as a result of cell cycle arrest by these compounds. The procedure was modified from the literature (Scott *et al.,* 2004). Cell cycle analysis was performed by flow cytometric evaluation of DNA content.

8.5 Materials and methods

8.5.1 Reagents

- RPMI and foetal calf serum
- RNase (Sigma-Aldrich)
- Propidium Iodide (PI) (Sigma-Aldrich)
- Phosphate buffered saline (PBS)
- Ethanol (100%) (Sigma-Aldrich)
- **Pg 8** (0.711 and 1.422 µM)
- [Au(dppe)$_2$]Cl (0.131 and 0.262 µM)

8.5.2 Cell lines and culture

Human T-cell lines (Jurkat) were cultured in RPMI 1640 supplemented with 10% v/v heat-inactivated FCS and 1% penicillin-streptomycin. Cells were incubated with the experimental compounds for 18, 24 and 48 hours at 37 ℃ and 5% carbon dioxide.

8.5.3. Flow cytometric analysis of cell cycle progression

Cells (1 x 10^5 cells/ml) were treated with [Au(dppe)$_2$]Cl and **Pg 8** for 18, 24 and 48h in cell culture flasks. After the incubation period, they were decanted from flasks and centrifuged for 5 min at 200 g. The cell pellet was re-suspended in 500 µl PBS and chilled on ice. The cold cell suspension was then added rapidly to flow cytometer tubes containing 500 µl of ice cold ethanol. Mixing was carried out by forcing air bubbles through the suspension and then kept on ice for 15 minutes. The cells were then centrifuged for 3 minutes at 300 g followed by suspension of the cell pellet in 125 µl of RNAse (2mg/ml 1.12% w/v sodium citrate). After incubation for 15 minutes at 37 ℃ in a water bath, 125 µl of PI was added to each tube and mixed well. Samples were allowed to stand for 30 minutes at room temperature before analysis by flow cytometry (Beckman Coulter FC 500). DNA histograms were collected and estimation of the percentages of cells in G_1, S and G_2/M was performed with a computer software program (Multicycle, Phoenix Flow systems, San Diego, CA).

8.5.4 Statistical methods

All assays were performed at least five times and all data are presented as ± S.E.M. Differences in the cell cycle profiles (G_0/G_1, S and G_2/M phases) of untreated and treated cells were also compared by ANOVA (2-way) followed by Bonferroni's Multiple Comparison Test (*Fig. 8.7*) . Significance was established at $P<0.05$. The treatment that was significantly different from the fresh, viable cells is denoted with an asterix (*).

8.6 Results and discussion

Representative histograms and graphs showing changes in the cell cycle profiles (G_0/G_1, S and G_2/M phases) after 18, 24 and 48 h with or without exposure to the experimental compounds are shown below (Fig 8.2-8.6).

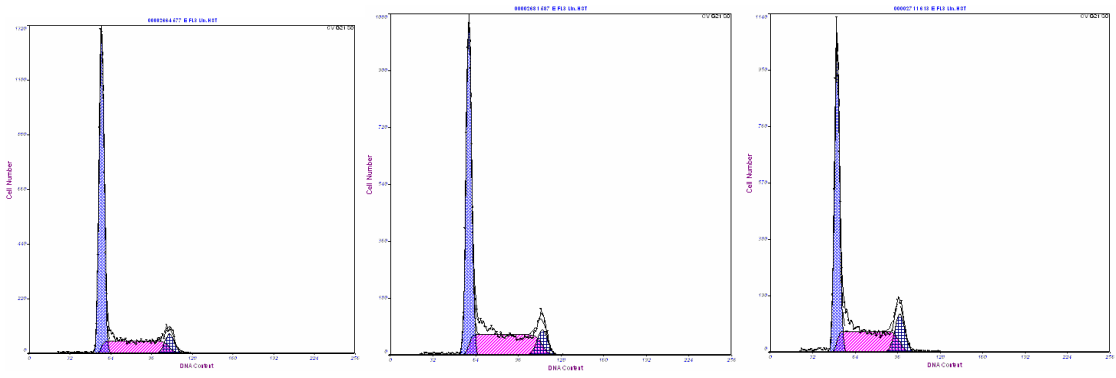

18 h 24 h 48 h

Fluorescence intensity (PI) representing cellular DNA content is indicated on *X* axis and cell count on the *Y*-axis

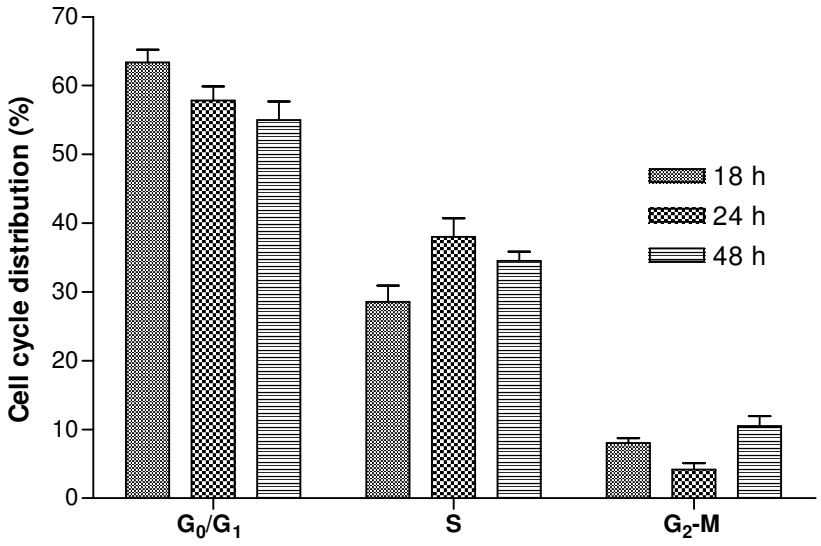

Fig. 8.2: Cell cycle progression of untreated Jurkat cells. Cells were incubated for 18, 24 and 48 hours without the experimental compounds. Cell cycle analysis was performed using flow cytometric evaluation of DNA content.

At 24 h, there was a decrease in the number of cells in G_1 phase (from 63 to 58%), which was complimented by a slight increase in the number of cells in the S-phase (from 29 to 38 %) (*Fig. 8.2*). At 48 h, there was a decrease in the S-phase (from 38 % to 35 %) and a marked increase in the G_2 phase (from 4 to 11%). The observed changes in the cell cycle progression of untreated cells were used to determine if any changes had occurred in the treated samples (*Fig. 8.3-8.6*).

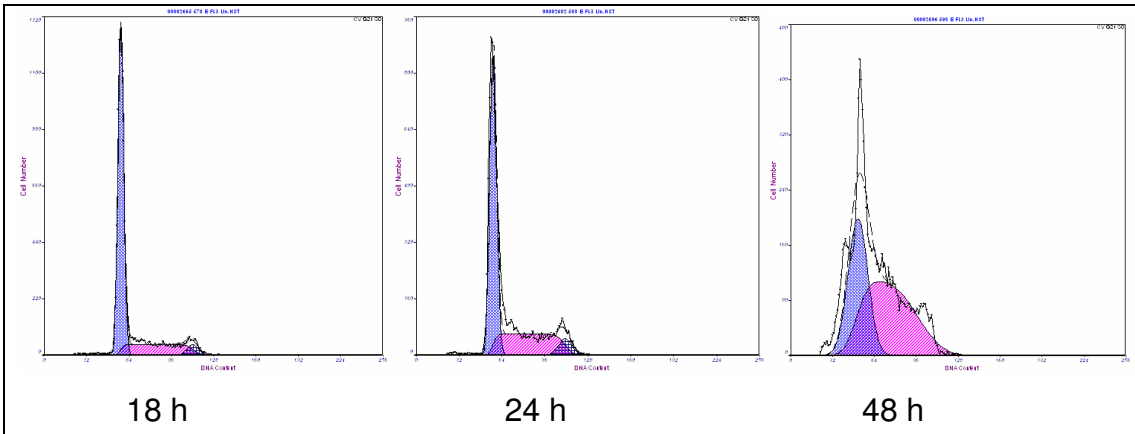

Fluorescence intensity (PI) representing cellular DNA content is indicated on *X* axis and cell count on the *Y*-axis

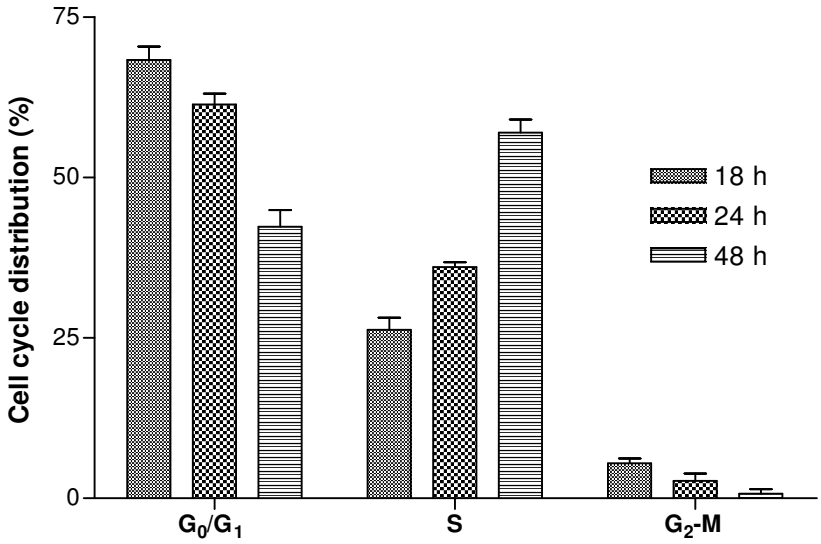

Fig. 8.3: Effect of 0.711 µM of **Pg 8** on the cell cycle progression of Jurkat cells after 18, 24 and 48 h treatment.

Cells exposed to 0.711 µM of **Pg 8** for 18 and 24 h did not exhibit any differences in cell cycle progression (*Fig. 8.3*). After 48 h, the number of cells in G_1 was significantly reduced (from 61 to 47%) with the subsequent accumulation of cells in S-phase (from 36 to 57%). Due to this blockade of the S-phase, G_2 phase contained virtually no cells (1%).

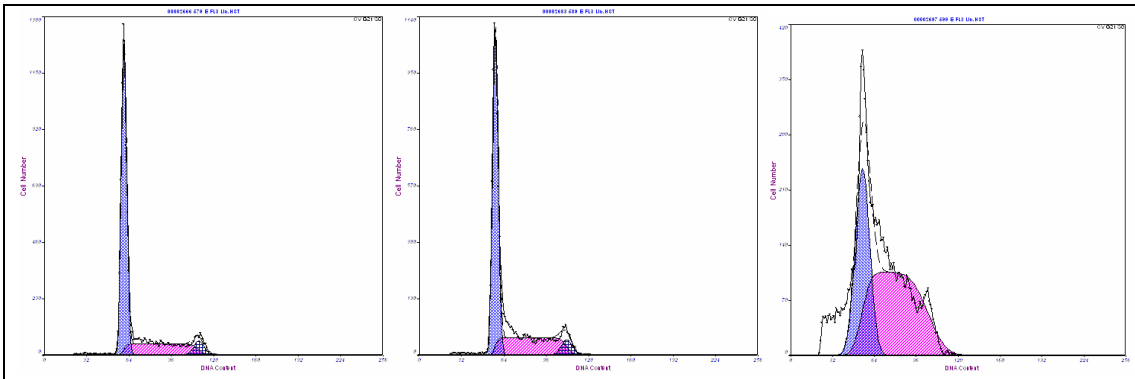

Fluorescence intensity (PI) representing cellular DNA content is indicated on *X* axis and cell count on the *Y*-axis

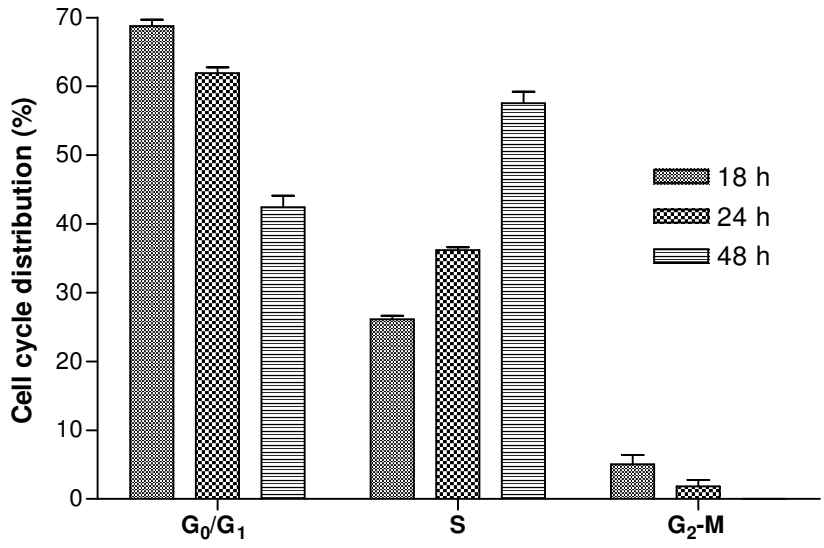

Fig. 8.4: Effect of 1.422 µM of **Pg 8** on the cell cycle progression of Jurkat cells after 18, 24 and 48 h treatment.

Cells exposed to 1.422 µM of **Pg 8** (*Fig. 8.4*) showed the same behaviour as the ones exposed to half the concentration (*Fig. 8.3*). After 48 h, the number of cells

in G_1 was significantly reduced (from 62 to 47 %) with the subsequent accumulation of cells in S-phase (from 36 to 58%). There were no cells in the G_2 phase.

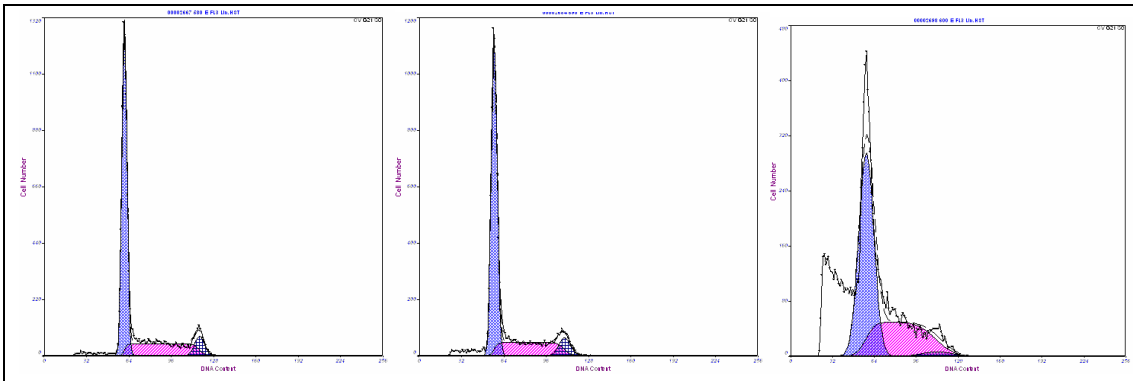

18 h 24 h 48 h

Fluorescence intensity (PI) representing cellular DNA content is indicated on *X* axis and cell count on the *Y*-axis

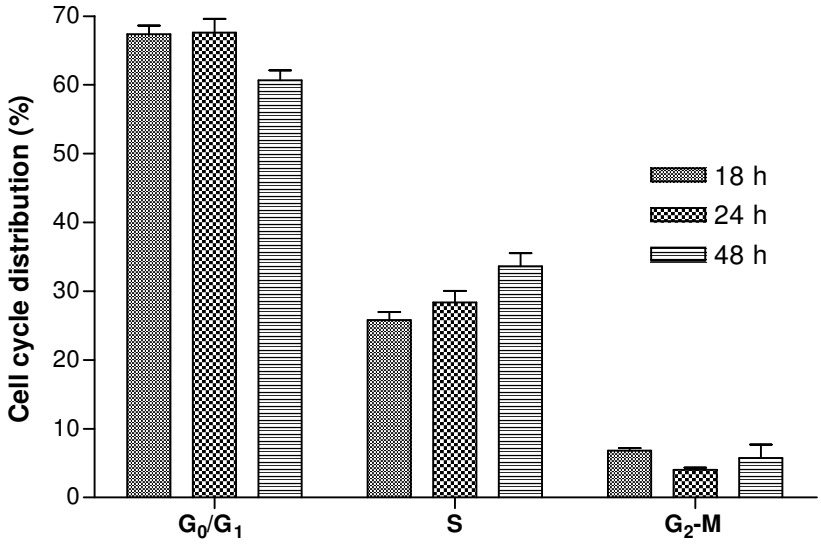

Fig. 8.5: Effect of 0.131 µM of $[Au(dppe)_2]Cl$ on the cell cycle progression of Jurkat cells after 18, 24 and 48 h treatment..

After exposure of Jurkat cells to $[Au(dppe)_2]Cl$ (0.131 µM) for 18 h and 24 h, no significant changes to progression of cell cycle were observed (*Fig. 8.5*). However, significant changes were observed after 48h. The number of cells in G_1

decreased from 68 to 61 % while there was an increase in S-phase (from 28 to 34%). The number of cells in G_2 phase increased insignificantly (from 4 to 5%).

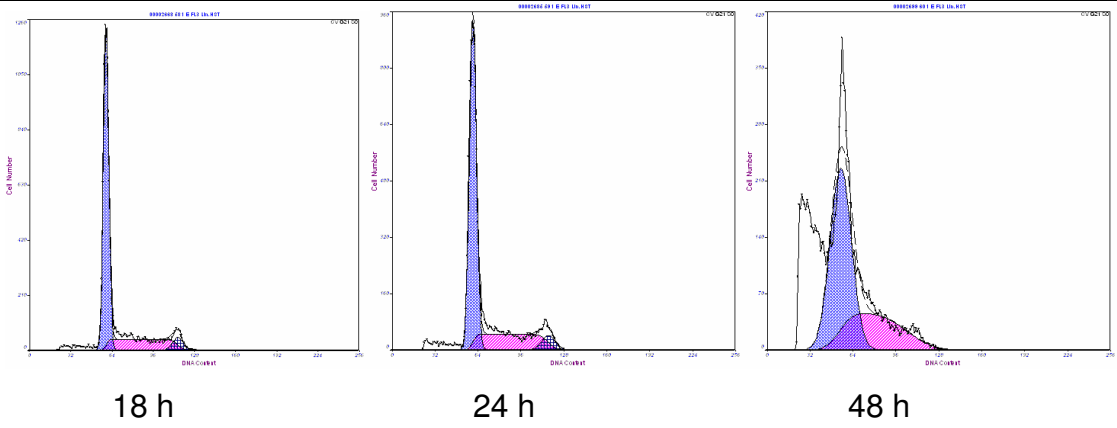

Fluorescence intensity (PI) representing cellular DNA content is indicated on *X* axis and cell count on the *Y*-axis

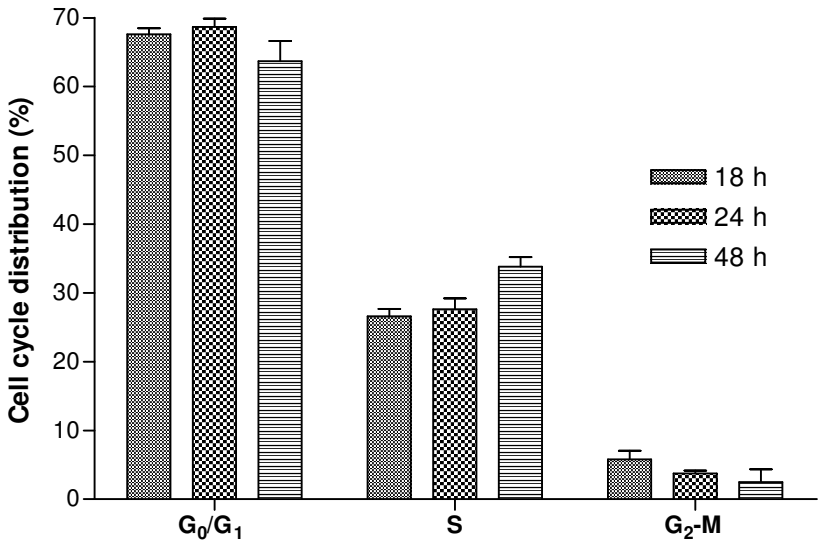

Fig. 8.6: Effect of 0.262 μM of $[Au(dppe)_2]Cl$ on the cell cycle progression of Jurkat cells after 18, 24 and 48 h treatment..

Cells exposed to 0.262 µM of $[Au(dppe)_2]Cl$ showed the same pattern as those exposed to half the concentration (*Fig. 8.6*). At 48 h, the number of cells in G_1 decreased from 69 to 64 % while S-phase increased from 28 to 34%. G_2 phase showed an insignificant decrease (from 4 to 3%).

The DNA histogram yields the relative number of cells in G_1/G_0, S, and G_2/M phases of the cell cycle (Ormerod, 2002). Although some information about cell cycle progression can be deduced by following changes in the cell cycle phases with time, it gives static information. For example, although it is possible to estimate the percentage of cells in S phase, the measurement does not directly tell whether those cells are still moving through the S phase. A very distinct connection has been forged between the cell cycle clock apparatus and apoptosis (Lundberg and Weinberg, 1999). The paclitaxel-induced apoptosis of human breast cancer cells has been found to depend upon the induction of the cdc2 kinase at the G_2/M phase transition of the cell cycle.

Comparison of untreated and treated cells at different time intervals showed significant changes (*Fig. 8.7*). At 18 h, cells treated with **Pg 8** (0.711 and 1.422 µM) showed an increase of cells ($P<0.05$) in the G_0/G_1 phase but there was no complimentary decrease in the number of cells in either the S or G_2 phase. After 24 h, only cells treated with $[Au(dppe)_2]Cl$ (0.130 and 0.262 µM) showed any changes in cell cycle progression. There was a significant increase ($P<0.01$) in the number of cells in the G_0/G_1 phase with a concomitant decrease in the number of cells in the S-phase. After 48 h, the treated cells showed significant differences in the cell cycle sequence. Cells treated with $[Au(dppe)_2]Cl$ (0.262 µM) had significantly larger number ($P<0.05$) of cells in G_0/G_1 phase than the untreated cells. However, this difference was not as large as that observed at 24 h. It is probable that $[Au(dppe)_2]Cl$ induced apoptosis was not necessarily as a result of cell cycle arrest.

In contrast, cell cycle progression at 48 h was greatly perturbed by **Pg 8**. The number of cells in G_1 phase was reduced by 15% while those in the S-phase increased by 22% at both concentrations ($P<0.01$). There were no cells detected in the G_2 phase due to this blockade in the S-phase. Taken together, these results indicate that **Pg 8** inhibited cellular proliferation of Jurkat cells via an S-phase arrest of the cell cycle following exposure for 48 h.

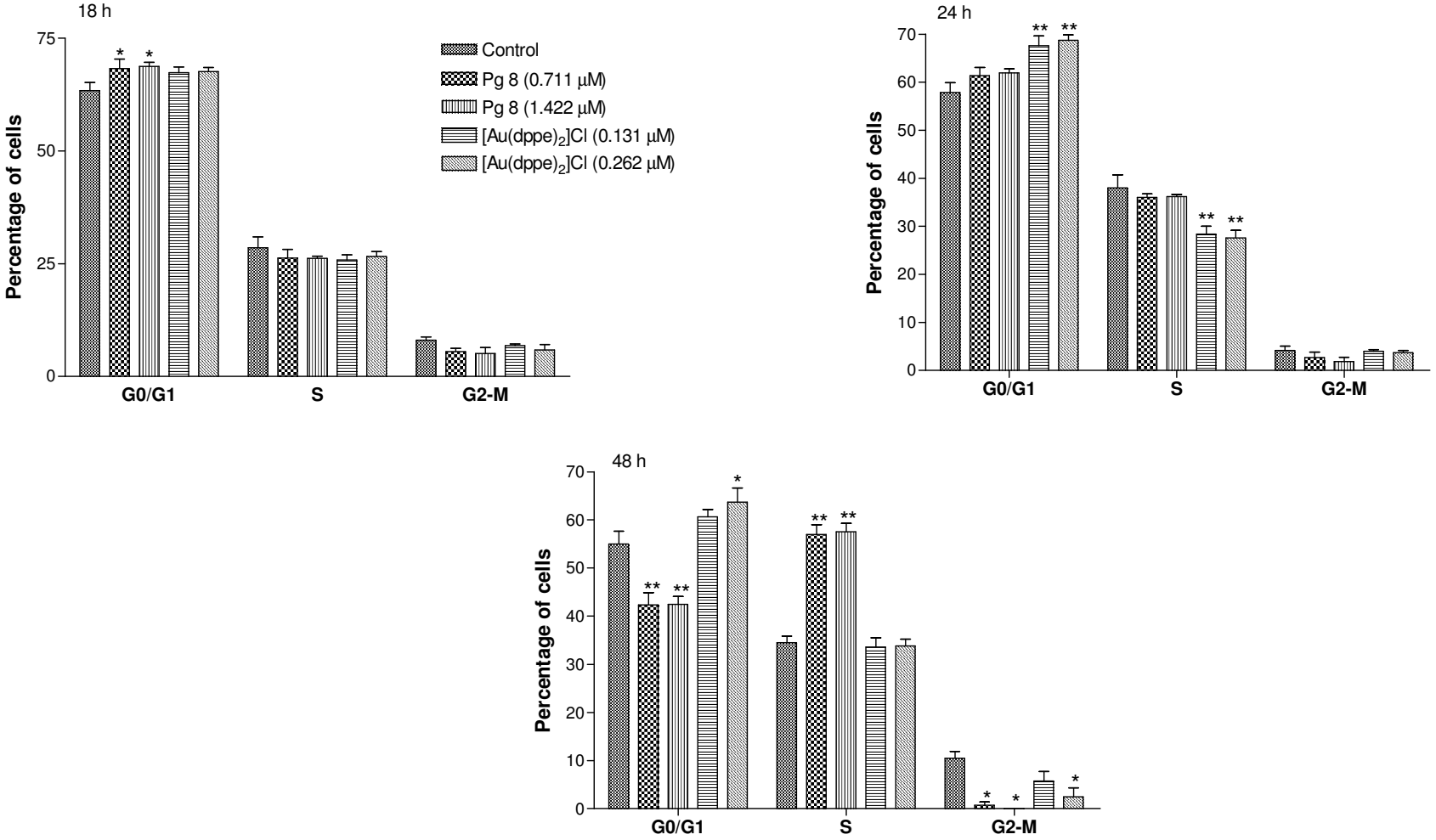

Fig. 8.7: Comparison of cell cycle progression of untreated Jurkat cells and those treated with **Pg 8** (0.711 and 1.422 M) and $[Au(dppe)_2]Cl$ (0.131 and 0.262 µM) after 18, 24 and 48 h. Differences in G_0/G_1, S and G_2/M phases of untreated and treated cells were compared by 2-way ANOVA. Significance was established at $P<0.05$.

Chapter IX

Uptake studies

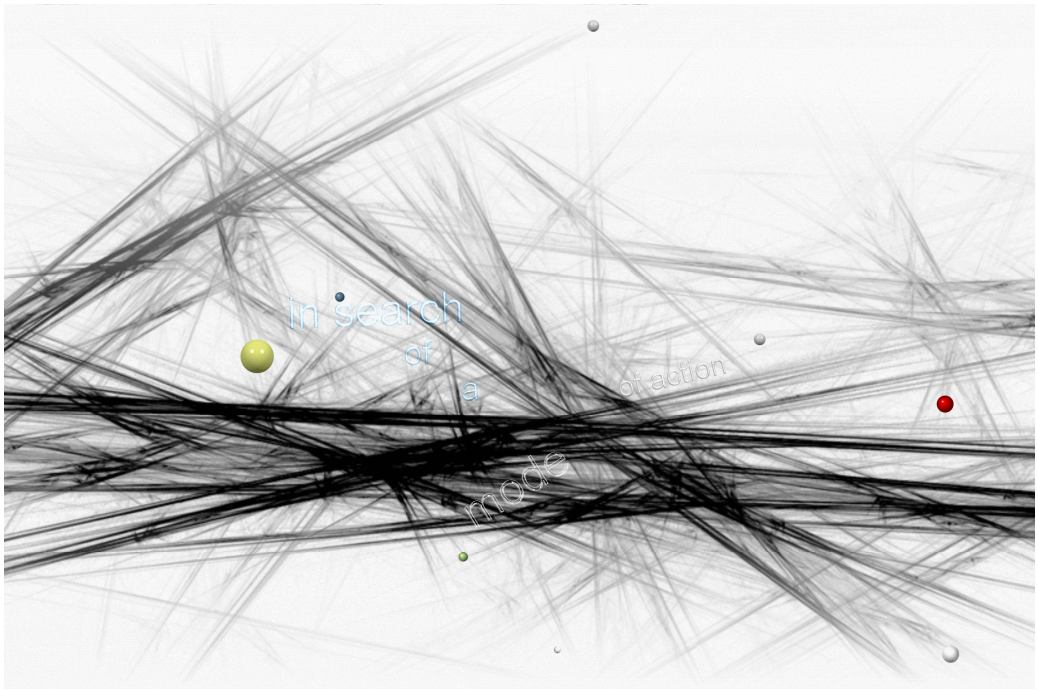

9.1 Introduction

The main cause of treatment failure and death of cancer patients is metastases- the formation of secondary tumours in organs distant from the original cancer (Zeevaart *et al.,* 2004). The effect of some anti-tumour agents is related to the extent of their penetration, accumulation and retention within tumour cells (Tsuruo *et al.,* 1982). The acquired resistance of tumour cells in some agents, a crucial problem in cancer chemotherapy, is related to intracellular drug accumulation and retention. Although therapeutic efficiency of the drug will also depend upon drug retention in the tumour and the ability of the molecules to cross cellular membranes, inefficient drug transfer from plasma to tissue can be a major impediment in achieving effective tumour chemotherapy (Artemov *et al.,* 2001).

One of the major, present-day uses of radiolabelled compounds in metabolic studies is in pre-clinical drug development (Billington *et al.,* 1992). The metabolism of the candidate-radiolabelled drug is studied from three standpoints: a) excretion studies b) tissue distribution and, c) formation of metabolites. Experiments on $[Au(dppe)_2]Cl$ in human plasma indicated that it was transferred relatively rapidly from plasma to red cells with an approximate half-life of 3 h at 25 ℃ (Berners-Price and Sadler, 1987b). After 18 h, 60% of the initial amount of $[Au(dppe)_2]Cl$ remained in the plasma. The 2-pyridyl and 4-pyridyl analogs of $[Au(dppe)_2]Cl$ were evaluated previously for anti-tumour activity in mice bearing i.p P388 leukaemia; whereas the 2-pyridyl complex had comparable activity to $[Au(dppe)_2]Cl$, the 4-pyridyl analog was inactive (Berners-Price *et al.,* 1999a). These differences may be related, at least in part, to differences in their uptake into cells as a consequence of their different hydrophilic character.

The assays discussed in this chapter aimed at determining the uptake and bio-distribution of the experimental compounds (^{103}Pd labelled $[Pd(d2pyrpe)_2][PF_6]_2$ and ^{198}Au labelled $[Au(dppe)_2]Cl$). These complexes provided a tool to follow the uptake into cells on an *in vitro* scale and the bio-distribution on an *in vivo* scale[6].

[6] The radioactivity was not expected to contribute to toxicity as much higher levels of radiation are required for that.

The test compounds were kindly synthesised at South African Nuclear Energy Corporation Ltd (NECSA) by Judith Wagener.

9.2 Preparation of ^{103}Pd labelled $[Pd(d2pyrpe)_2][PF_6]_2$

9.2.1 Irradiation of Na_2PdCl_4

Na_2PdCl_4 (94 mg, 0.32 mmol) was irradiated for 3.5 days. According to Origen™ calculations, the combined dose rates for ^{103}Pd and ^{109}Pd was equal to 13 mCi for 100 mg Na_2PdCl_4 after 3.5 days irradiation at a thermal neutron flux of 1.79×10^{14} $n.cm^{-2}.s^{-1}$ in the hydraulic position, BE-1 or BW-1 in SAFARI-1.

9.2.2. Preparation of $[Pd(d2pyrpe)_2]Cl_2$

An activity of 1.77 mCi was read on the Capintec (Pd-103 calibration factor = 562 X 10) (extrapolated value from Origen™ S calculation 2.59 mCi). The activated Na_2PdCl_4 (84.6 mg, 0.288 mmol) was transferred to a vial (activity of 1.488 mCi Pd-103). A total volume of ±7 ml THF was added to the palladium salt. The ligand (d2pyrpe) (262.09 mg, 0.64 mmol) was weighed (under argon) and added as a solid to the stirred solution of Na_2PdCl_4. The mixture was stirred for 12 hrs at room temperature to yield a yellow-green precipitate. The excess THF was extracted with a syringe and the yellow precipitate dried *in vacuo.* Crude Yield: 216.09 mg (76.4%).

9.2.3 Preparation of $[^{103}Pd(d2pyrpe)_2][PF_6]_2$

NH_4PF_6 (68.66 mg, 0.418 mmol) was added to a stirred solution (8 ml of acetone) of $[Pd(d2pyrpe)_2]Cl_2$ (205.29 mg, 0.209 mmol). After stirring for 45 min, the yellow-green suspension turned grey in colour. A syringe was packed with Celite 545 (Kieselgur) (a Teflon frit was placed at the bottom and top of the celite). The filter medium was washed with 5 ml acetone and additional 2 X 5 ml fractions. The reaction mixture was filtered through the celite column. The celite was washed with 2 X 2ml acetone. Slight pressure was introduced with the syringe plunger and the combined fractions of the clear pale yellow filtrate were reduced to ~2 ml with an aspirator.

Ether (4 ml) was added to the filtrate and a white/cream precipitate was formed. The precipitate was washed twice with ether (1 ml) and the excess solvent was extracted with a syringe. The product was then dried *in vacuo* for 30 min. Activity on the Celite column was high relative to the acetone filtrate containing the product and this may have been contributed by Cl-36 of NH_4Cl that had formed and was retained. According to a similar procedure using non-irradiated Na_2PdCl_4, 60% yield was obtained and therefore it was assumed that 170 µCi = 60% product (150 mg). The final specific activity was 1.133 µCi/mg.

9.3 Preparation of ^{198}Au labelled $[Au(dppe)_2]Cl$

All manipulations were carried out under an inert atmosphere (argon).

9.3.1 Irradiation of Au-metal

The radioactive experiment was carried out with activated Au (41.9 mg) and non-irradiated Au (30.5 mg) for the synthesis ClAuTHT (the precursor for $[Au(dppe)_2]Cl$). Gold was activated for 10 min in the hydraulic B-position.

9.3.2 Preparation of $HAuCl_4.4H_2O$

680 µl HCl/HNO_3 (3:1) was added to a vial containing activated gold (41.9 mg) and non-irradiated gold (30.5 mg, 0.368 mmol). 18.15 mCi was read on the Capintec (Au-198 calibration factor = 149). The vial was placed inside a lead pot on a hotplate (45°C) while stirring and covered with a test tube (serving as a watch glass) to minimise evaporation of the acid. This dissolution step took approximately 2 h. The aqua regia was evaporated by increasing the temperature to 50°C while blowing argon into the vial (60-90 min). The yellow residue was washed with HCl (650 µl) followed by H_2O (650 µl) and dried at 50°C after each addition. The products' activity was 19.2 mCi and a yield of 100% was assumed.

9.3.3 Preparation of ClAuTHT

$HAuCl_4.4H_2O$ was dissolved in 900 µl $EtOH/H_2O$ (5:1) and the insoluble particles were removed by filtration through a Millex GP 0.22 µm filter. The filter was rinsed 3 times with additional $EtOH/H_2O$. The combined filtrate was evaporated to ±1000 µl and the activity of $HAuCl_4.4H_2O$ was 16.7mCi.

The vial was sealed and an argon needle was inserted followed by a vent-needle. THT (600 µl) was added dropwise to $HAuCl_4.4H_2O$. The mixture was stirred for 15 min followed by extraction of the solution with a syringe. The remaining white precipitate was washed twice with ethanol (500µl) and extracted as described above. The precipitate was dried under vacuum and dissolved in a minimum volume of chloroform (calculated as 12.3 mg/ml $CHCl_3$).).

9.3.4 Preparation of [^{198}Au(dppe)$_2$]Cl

2.93 µl of $ClAuTHT/CHCl_3$ (3.6 mg; 0.011 mmol) was evaporated and dppe (8.84 mg, 0.022 mmol) in THF (1 ml) was added to it. The reaction mixture was stirred for 15 min (a precipitate formed after stirring for 7 min). The white precipitate was then dried *in vacuo*.

9.4 Uptake of [^{103}Pd(d2pyrpe)$_2$][PF_6]$_2$ and [^{198}Au(dppe)$_2$]Cl by Jurkat cells

The procedure for the determination of the uptake and distribution of [^{103}Pd(d2pyrpe)$_2$][PF_6]$_2$ and [^{198}Au(dppe)$_2$]Cl in Jurkat cells was modified from the literature (Tsuruo *et al.,* 1982).

9.5 Materials and methods

9.5.1 Reagents

- RPMI and foetal calf serum
- Phosphate buffered saline (PBS)
- ^{103}Pd labelled [Pd(d2pyrpe)$_2$][PF_6]$_2$ (**Pg 8**)- 5 and 10 µM in DMSO
- ^{198}Au labelled [Au(dppe)$_2$]Cl- 5 and 10 µM in DMSO

9.5.2 Cell lines and culture

Human T-cell lines (Jurkat) were cultured in RPMI 1640 supplemented with 10% v/v heat-inactivated FCS and 1% penicillin-streptomycin. The cell culture was maintained at 37 °C and 5% CO_2.

9.5.3 Experimental procedure

200 µl of radiolabelled $[Pd(d2pyrpe)_2][PF_6]_2$ and $[Au(dppe)_2]Cl$ (both at a concentration of 5 and 10 µM) were added to test tubes containing a suspension (1,800 µl) of Jurkat cells (5 x 10^6 cells/ml). The mixture was incubated while mixing at 37 °C (+ 5% CO_2) for 1 hr. After incubation, the cells were centrifuged at 800 g (2000 rpm TJ 6) for 10 min. The supernatant was poured into new, clean, marked 5 ml test tubes (kept separately). The pellet was resuspended in PBS (3 ml) and centrifuged as before. The PBS was poured into new, clean, marked 5 ml test tubes and keep separately. The tubes were counted separately using 1261 multigamma manual gamma counter (LKB Wallac).

9.5.4 Statistical methods

Cells from eight different cell culture flasks were used for these assays. The activity that was obtained from the experiments was determined from counts per minute (CPM). Hence this represented the amount of compound distributed either in the supernactant or cell. Statistics was carried out on Graphpad™ and One Way Analysis of Variance (ANOVA) followed by Bonferroni's Multiple Comparison Test to determine significance between the two experimental compounds in the cells and/or supernactant. $P < 0.001$ was considered significant.

9.6 Results and discussion

The distribution of the radiolabelled compounds in Jurkat cells after 1 h is presented in Fig 9.1.

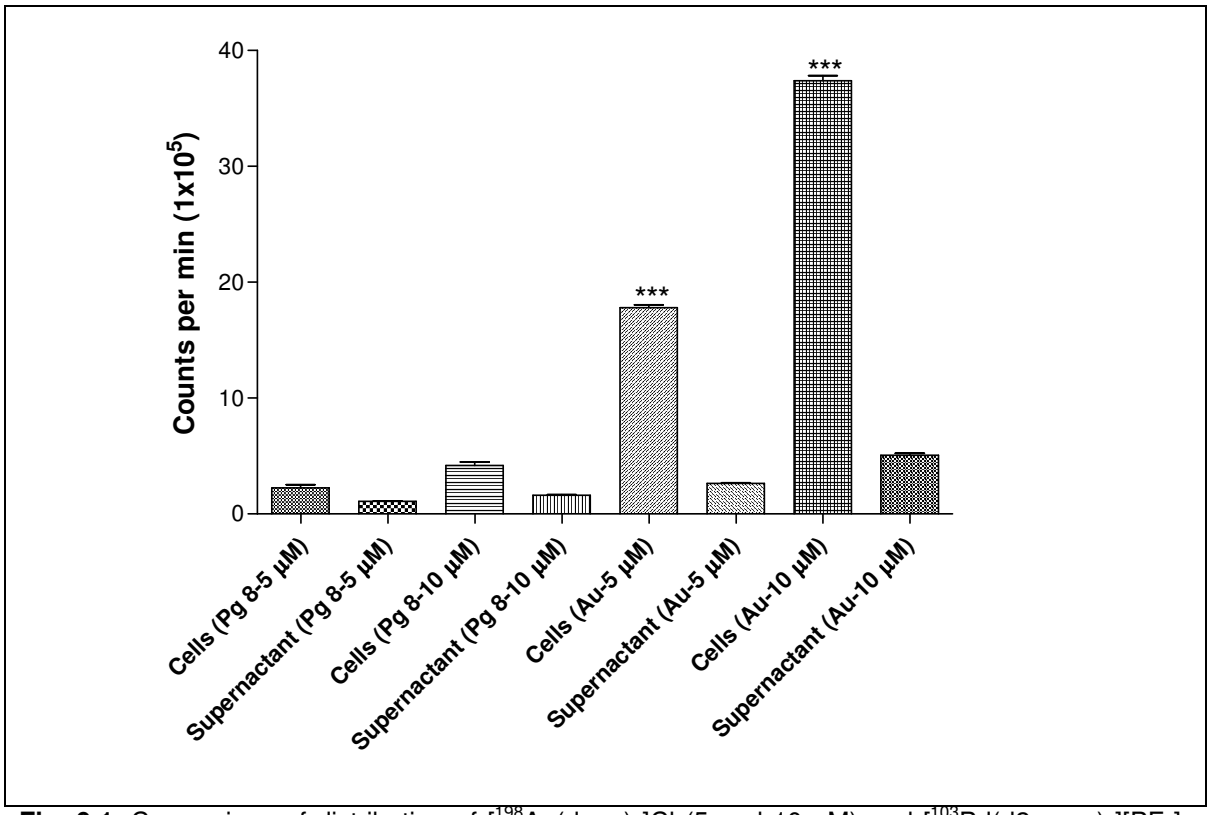

Fig. 9.1: Comparison of distribution of $[^{198}Au(dppe)_2]Cl$ (5 and 10 µM) and $[^{103}Pd(d2pyrpe)_2][PF_6]_2$ (5 and 10 µM) in Jurkat cells after exposure for 1 h. The results shown here were obtained from an average of 8 different cell populations and the values are means ±SEM.

In general, there was a significant difference ($P< 0.001$) between the amounts of compound taken up into the cells when compared to the amount left in the supernactant for both complexes. After incubation for 1h, $[^{198}Au(dppe)_2]Cl$ (5 and 10 µM) was taken up into the cells at significantly larger amounts ($P< 0.001$) than $[^{103}Pd(d2pyrpe)_2][PF_6]_2$ (5 and 10 µM). This large difference in uptake may be as a consequence of lipophilicity. The former compound was found to be more lipophilic (log $P= 0.362$) than the former (log $P= -0.093$) and hence able to pass through the lipid layers of cells more rapidly.

In both compounds, the higher concentration (10 µM) was found to accumulate in larger amounts ($P< 0.001$) than the lower concentration (5 µM). Uptake studies of [^{14}C][Au(dppe)$_2$]Cl by isolated rat hepatocytes showed that rapid maximal uptake took place within 30 min (Smith *et al.,* 1989). The amount of radiolabelled drug associated with hepatocytes was also concentration-dependent. The authors proposed that the mechanism by which [Au(dppe)$_2$]Cl gained access to the intracellular compartments was most likely linked to its lipid solubility. In other experiments, NMR studies showed that nearly half of the [Au(dppe)$_2$]Cl added to plasma was transferred into cells (Berners-Price and Sadler, 1987b). Experiments on red cell ghosts confirmed that the complex can bind intact in the membrane.

9.7 Biodistribution of [^{103}Pd(d2pyrpe)$_2$][PF$_6$]$_2$ and [^{198}Au(dppe)$_2$]Cl in rats

This study was carried out by Judith Wagener and Dr Jan-Rihn Zeevaart (NECSA) at the University of Pretoria Biomedical Research Centre (UPBRC). Animal experimentation was done according to the National Code for the Handling and Use of Animals in Research, Education, Diagnosis and Testing of Drugs and Related Substances in South Africa. Ethical approval by the AUCC (Animal Use and Care Committee) was obtained (Protocol No. H1206) and the study was done according to the rules and regulations laid down by the International Controlling Body for Radioisotope Studies.

9.7.1 Formulations

- [^{103}Pd(d2pyrpe)$_2$][PF$_6$]$_2$ (75 mg) was dissolved in DMSO (140 µl), ethanol (800 µl) and H_2O (3200 µl). The filtered 4000 µl fraction had an activity of 3 µCi. An injection volume of 450 µl and an activity of 0.3 µCi was used (7.5 X 10^{-4} µCi/µl).

- [^{198}Au(dppe)$_2$]Cl (11.43 mg) was dissolved in ethanol (1200 µl) and H_2O (7200 µl) and 3 ml of the solution was filtered (Millex GP 0.22 µm). An injection volume of 500 µl and an activity of 25 µCi were used (5.0 X 10^{-2} µCi/µl).

9.7.2 Experimental animals

Adult male Sprague Dawley rats (six rats per compound) were used to follow the biodistribution on a gamma camera. The animals were kept in separate cages and fed a balanced diet and water *ad libitum*.

9.7.3 Experimental design

On the day of the experiment, the animals were anaesthetised by an intraperitoneal (i.p.) injection of 6 % sodium pentobarbitone solution at a dose of 1 ml/kg. A 24 G jelco was inserted into the tail vein of the animals to administer the radiolabelled compounds. The rats were each injected with an extremely low, non-toxic dosage of radio labelled compound (^{198}Au labelled [Au(dppe)$_2$]Cl and ^{103}Pd labelled [Pd(d2pyrpe)$_2$][PF$_6$]$_2$). Animals were screened from time to time to monitor the realisation of steady state bio-distribution.

Two animals per group were scanned in parallel with an Elscint Gamma Camera at the Diagnostic Imaging unit at UPBRC in order to obtain the radionuclide imaging. Two minute static studies were performed every half an hour up to 6 hours. Isoflurane was used to immobilize the animals for the 2 minute static studies. The animals were sacrificed using an isoflurane overdose after a six hour period. The organs were separated and counted in a well type counter at NECSA [Canberra Model uniSPEC Universal MCA (Multichannel Analyzer) system with Canberra 3" x 3" NaI(TL) well detector]. From the organ counts as well as the reference activity in a syringe, the %ID/g (Injected Dose/gram) was calculated.

9.7.4 Statistical methods

Statistics was carried out on Graphpad™ and One Way Analysis of Variance (ANOVA) followed by Bonferroni's Multiple Comparison Test to determine significance between the two experimental compounds in the organs. $P < 0.001$ was considered significant.

9.8 Results and discussion

In interpreting the *in vivo* results, it must be kept in mind that only the distribution of the radio-nuclide entity of the complex is observed; which is not necessarily the same as the radio-nuclide-ligand complex that has been administered, due to possibilities of *in vivo* transchelators (Zeevaart *et al.,* 2001). The biodistribution at 6 h (expressed as percentage of injected dose per gram of organ) of the radiolabelled compounds is presented in Fig 9.2.

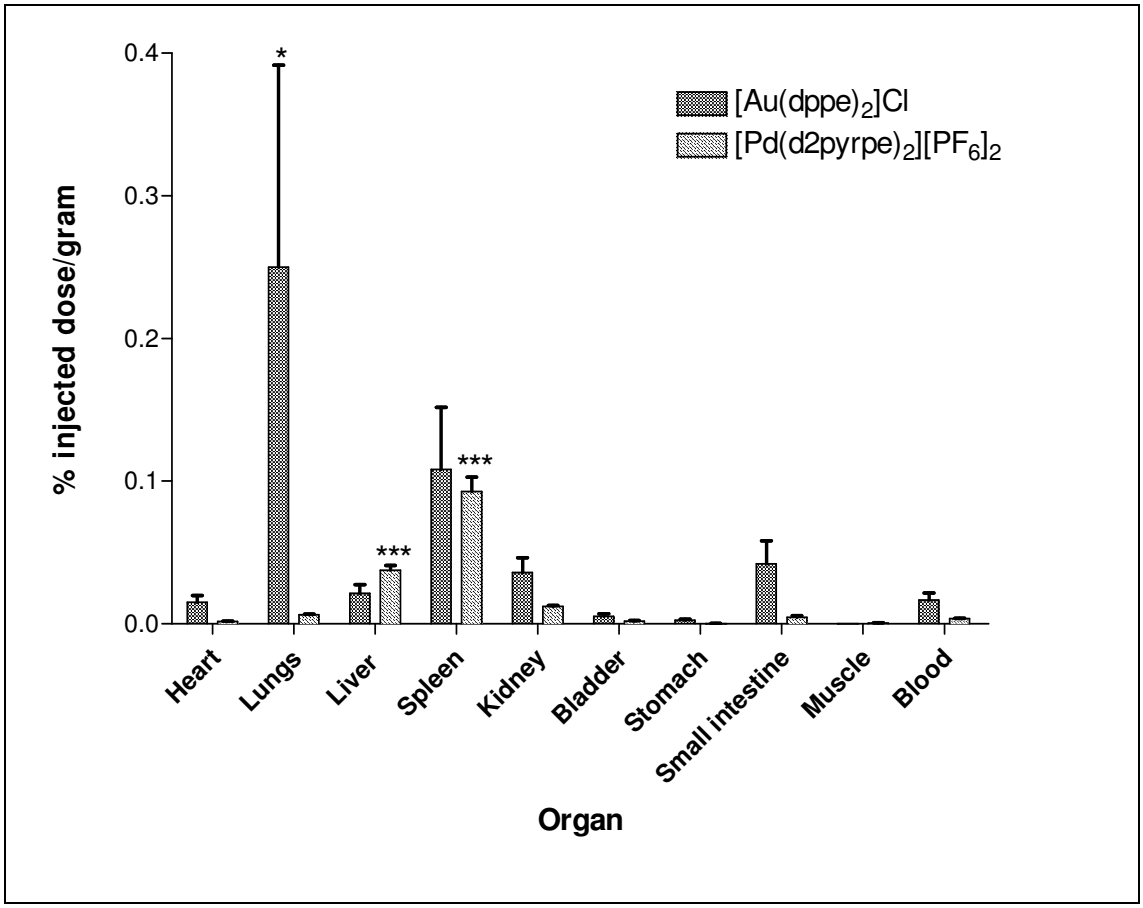

Fig. 9.2: Biodistribution of selected organs of adult male Sprague Dawley rats as expressed as a percentage of injected dose per gram of [^{198}Au(dppe)$_2$]Cl and [^{103}Pd(d2pyrpe)$_2$][PF$_6$]$_2$.at 6 h. Illustrated values are means ±S.E.M.

The biodistribution showed predominantly high reticulo-endothelial uptake for the two compounds. In terms of the total uptake it was found that [^{198}Au(dppe)$_2$]Cl which is more lipophilic was taken more efficiently in organs than [^{103}Pd(d2pyrpe)$_2$][PF$_6$]$_2$ which is less lipophilic. These findings correlate to the

results obtained from *in vitro* uptake studies carried out on Jurkat cells (Section 9.6).

[^{198}Au(dppe)$_2$]Cl accumulated significantly ($P< 0.05$) in the lungs followed by the spleen, small intestine and liver, while [^{103}Pd(d2pyrpe)$_2$][PF$_6$]$_2$ was mostly taken up in the spleen followed by the liver. The amount of [^{103}Pd(d2pyrpe)$_2$][PF$_6$]$_2$ that accumulated in the spleen and liver was significantly higher ($P< 0.001$) than that found in the rest of the organs. The liver organ mainly traps neutral and positively charged molecules (Zeevaart *et al.,* 2004).

In comparing the biodistribution of the two compounds in similar organs, it was found that the amounts taken up were not significantly different apart from that observed in the lungs. The amount of [^{198}Au(dppe)$_2$]Cl accumulated in the lungs was much higher than that of [^{103}Pd(d2pyrpe)$_2$][PF$_6$]$_2$ ($P< 0.001$). In summary, while the gold compound seemed to accumulate in most organs, most of the palladium compound appears to have been excreted. [^{103}Pd(d2pyrpe)$_2$][PF$_6$]$_2$ showed similar behaviour to that of hydrophilic drugs, which are expected to have limited bio-distribution (as compared to lipophilic drugs). This might imply a more selective tumour uptake since it does not show a tendency to accumulate in the body.

Chapter X

Acute toxicity studies

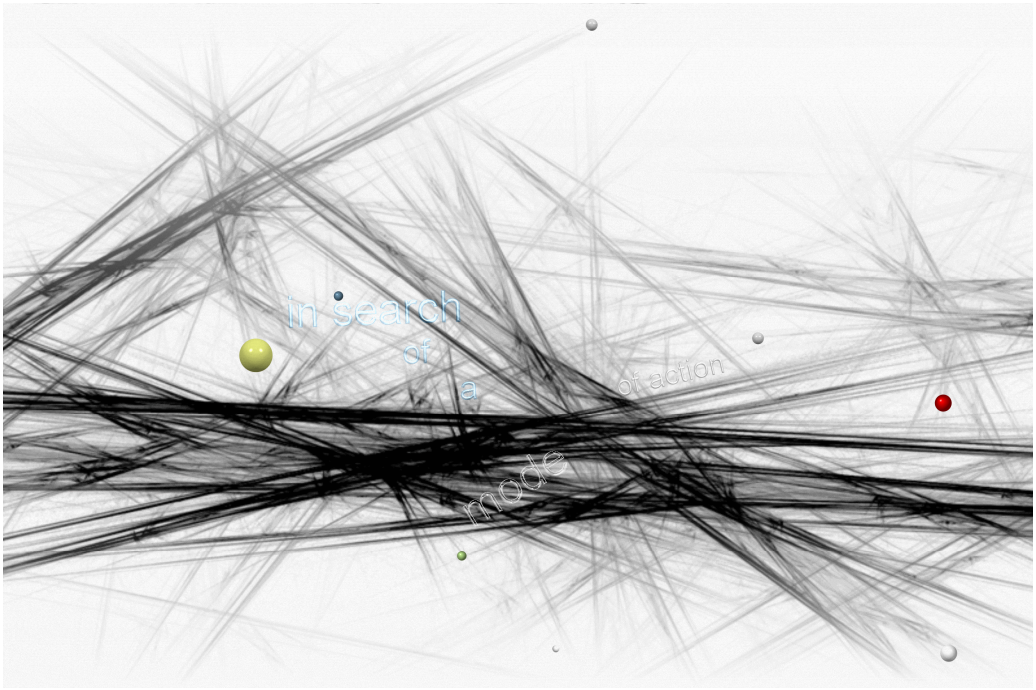

10.1 Introduction

In the process of drug discovery, selected active substances are further differentiated according to their toxicity (Popiolkiewicz *et al.,* 2005). It is desired to find not only the most active, but also the least toxic substances as well. Toxicity studies on animals, which must be conducted before planning any clinical trial, constitute an important part of the whole drug discovery process. Acute toxicity studies are conducted in animals to ascertain the total adverse biological effects caused during a finite period of time following administration of a single, frequently large dose of an agent (or several doses repeated over a short interval of time) (Ecobichon, 1997).

The definition of hepatotoxicity is based on biological parameters (elevation of alkaline phosphatase enzyme (ALT, AST and GGT) or on clinical abnormalities (hepatitis, jaundice) (Ozcanli *et al.,* 2006). The degree of damage to the tissue or whole body, respectively, can be assessed by specific tests of enzymes (Conková *et al.,* 2005). In clinical diagnostics, determination of transaminases is of great importance. In the rat, ALT is chiefly a liver specific enzyme while AST has a ubiquitous tissue distribution (Elovaara *et al.,* 2007). Increased plasma levels of ALT are therefore attributed to liver damage but those of AST may imply damage to organs other than the liver. The absence of any notable increases in plasma ALP and GGT indicate that there are no marked changes involving the biliary system. A lot of medications may induce a clinical or biological hepatic toxicity and they need to be carefully supervised (Ozcanli *et al.,* 2006).

The influence of the route of administration of $[Au(dppe)_2]Cl$ on its activity against i.p. P388 leukaemia was investigated (Berners-Price *et al.,* 1986). The complex was less toxic when given i.v., s.c. or p.o. but was inactive in this tumour system by these three routes of administration. Preliminary toxicological studies on $[Au(dppe)_2]Cl$ revealed some local toxicity after sub-cutaneous administration, and pulmonary toxicity after intravenous injection (Berners-Price and Sadler, 1987b). It is possible that these effects could be related to the apparent disruption of lipoprotein structures which was observed *in vitro*. The maximum tolerated dose

of the ligand (dppe) was found to be 50 µmol/kg and it was shown to be active in these tumour models also (Berners-Price *et al.,* 1987c).

In a preclinical evaluation of its toxicity, $[Au(dppe)_2]Cl$ produced toxicity in the liver, heart and lung in male beagle dogs (Smith *et al.,* 1989). After a single *i.v* administration of the compound (272 mg/m^2), serum aspartate aminotransferase, alanine aminotransferase and alkaline phosphatase activities were elevated markedly within 48 hr. Histopathologic evaluation revealed multiple, focal areas of necrosis distributed throughout all zones of the liver. Additionally, $[Audppe)_2]Cl$, an effective chemotherapeutic agent in animal models of neoplasia was cardiotoxic to rabbits (Hoke *et al.,* 1989). This resulted in scattered zones of subendocardial and myocardial cellular necrosis and mineralization, along with areas of contraction band necrosis. Non-specific binding to proteins or other macromolecules might explain the high host toxicity associated with very lipophilic cations such as $[Audppe)_2]Cl$ (McKeage *et al.,* 2000).

.

10.2 Motivation for the study

In vitro results of $[Au(dppe)_2Cl]$ and $[Pd(d2pyrpe)_2][PF_6]_2$ (**Pg 8**) showed that the latter exhibited more selectivity than the former. The expected outcome was that the toxicity of the novel compound $[Pd(d2pyrpe)_2][PF_6]_2$ (**Pg 8**) would be lower than that of $[Au(dppe)_2]Cl$ (i.e,. higher maximum tolerated dose).

10.3 Aim

This study was carried out in order to establish the maximum tolerated dose (MTD) of $[Pd(d2pyrpe)_2][PF_6]_2$ (**Pg 8**) in mice.

10.4 Materials and Methods:

Ethical approval by the AUCC (Animal Use and Care Committee) was obtained (Protocol No. H1706). The study was conducted at the University of Pretoria

Biomedical Research Centre (UPBRC) from 24-29 August, 2006 and 22-27 September 2006.

10.4.1 Animals

Inbred female Balb/C mice of 6-8 weeks were used and housed individually in standard mouse cages in rooms with controlled environmental conditions. The animals were fed normal pellets (EPOL) and water *ad libitum*.

10.4.2 Sample size, dosage and route of administration

The study was carried out in two phases with 4 groups of 6 mice each being used per phase (total of 48 mice). The maximum tolerated dose of $[Au(dppe)_2]Cl$ was 3.0 µmol/kg/day for 5 days (Berners-Price *et al.,* 1990) and hence this concentration was used as a guideline. The weight of the mice was determined to adapt the dosages according to their body weight. The novel compound $[Pd(d2pyrpe)_2][PF_6]_2$ (**Pg 8**) and $[Au(dppe)_2]Cl$ (standard) were dissolved in analytical quality ethanol, with subsequent addition of water to make up a final dose volume of 0.5 ml and a concentration of ~5% ethanol. The dosages were prepared immediately prior to each i.p administration. $[Au(dppe)_2]Cl$ was soluble in ethanol while **Pg 8** (15 µmol/kg) was sparingly soluble. Solubility was achieved by sonication for 15 minutes. However both compounds precipitated out slightly and were mixed prior to injection.

A summary of the number of animals and dosages used in both phase 1 and phase 2 is shown below (*Table 1 and 2*)

Table10.1: Summary of dosages used in Phase 1 of the acute toxicity study carried out on Balb/c mice

	Control group	**Dose 1**	**Dose 2**
$[Au(dppe)_2]^+$	Ethanol-water solution 0.5 ml daily from day 1 to 5 administered to **6 mice** (5% ethanol)	3.0 µmol/kg daily from day 1 to 5 administered to **6 mice** (5% ethanol)	
Pg 8		3.0 µmol/kg daily from day 1 to 5 administered to **6 mice** (5% ethanol)	6.0 µmol/kg daily from day 1 to 5 administered to **6 mice** (5% ethanol)

Table 10.2: Summary of dosages used in Phase 2 of the acute toxicity study carried out on Balb/c mice

	Control group	**Dose 1**	**Dose 2**
$[Au(dppe)_2]^+$	Ethanol-water solution 0.5 ml daily from day 1 to 5 administered to **6 mice** (5% ethanol)	6.0 µmol/kg daily from day 1 to 5 administered to **6 mice** (5% ethanol)	
Pg 8		12.0 µmol/kg daily from day 1 to 5 administered to **6 mice** (5% ethanol)	15.0 µmol/kg daily from day 1 to 5 administered to **6 mice** (5% ethanol)

10.4.3 Duration of study

The total duration of the study was 10 days and each group of mice was injected i.p. every day for 5 days. For Phase 1, the ethanol-water solution and the first and second dosages of 3 µmol/kg and 6 µmol/kg were administered each day from day 1 to 5. Phase 2 followed whereby the ethanol-water solution and the third and fourth dosages of 6 mol {$[Au(dppe)_2]Cl$} and 12 µmol/kg and 15 µmol/kg (**Pg 8**) were administered every day from day 1 to 5. At the end of the study, the mice were weighed followed by anaesthetisation via isoflurane inhalation. Maximum blood was drawn via cardiac puncture while they were at the surgical plane of anaesthesia. Finally, the animals were further exposed to isoflurane until death occurred. Mice in Phase 2 category were dissected and major organs (liver, heart and kidneys) were weighed.

10.4.4 Evaluation of pain and distress

Body weights were recorded immediately prior to dosing (on day 1) so that an objective monitoring of weight could be done, indicating food intake, which is a good measure of animal well-being. The animals were also monitored for pain and stress (behavioural changes) immediately after the injection.

10.4.5 Chemical analysis

A whole blood profile was carried out on all the blood samples by the Department of Clinical Pathology at the Faculty of Veterinary Science (University of Pretoria). Standard liver enzymes (AST and GGT) were also analysed as well as levels of serum creatinine. Toxicity was to be established if adverse effects were observed on the experimental animals or if there was elevation of liver enzymes.

10.4.6 Statistical Analysis

Statistical analysis on levels of AST, GGT and creatinine was done on Graphpad™ by One Way Analysis of Variance (ANOVA) followed by Bonferroni's Multiple Comparison Test. Significance was indicated if $P < 0.05$.

10.5 Results and discussion

Acute toxicities of $[Au(dppe)_2]Cl$ and **Pg 8** were investigated in mice after i.p administration for 5 days. On the second day of the study (in both phases), mice injected with the former compound emitted squeaking sounds upon injection. This sign of discomfort was not observed for the remainder of the study.

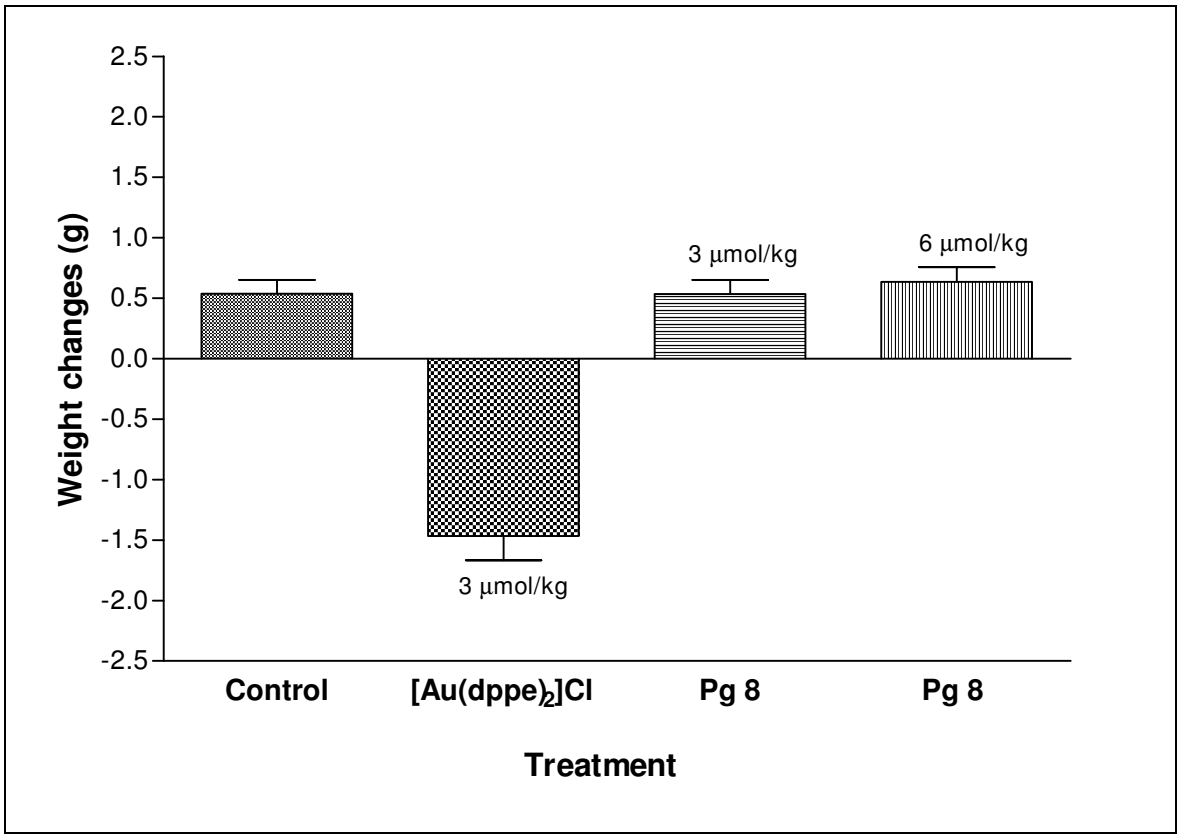

Fig.10.1: Mean body weight changes of control mice and mice treated with $[Au(dppe)_2]Cl$ (3 µmol/kg) and **Pg 8** (3 and 6 µmol/kg) in Phase 1 study.

In Phase 1, the average weight change in the control and **Pg 8** (3 and 6 µmol/kg) groups were comparable (2.6, 2.63 and 3.1 %) (*Fig. 10.1*). However, the animals

in the $[Au(dppe)_2]Cl$ (3 µmol/kg) group lost an average of 7.6 % of their total body weight.

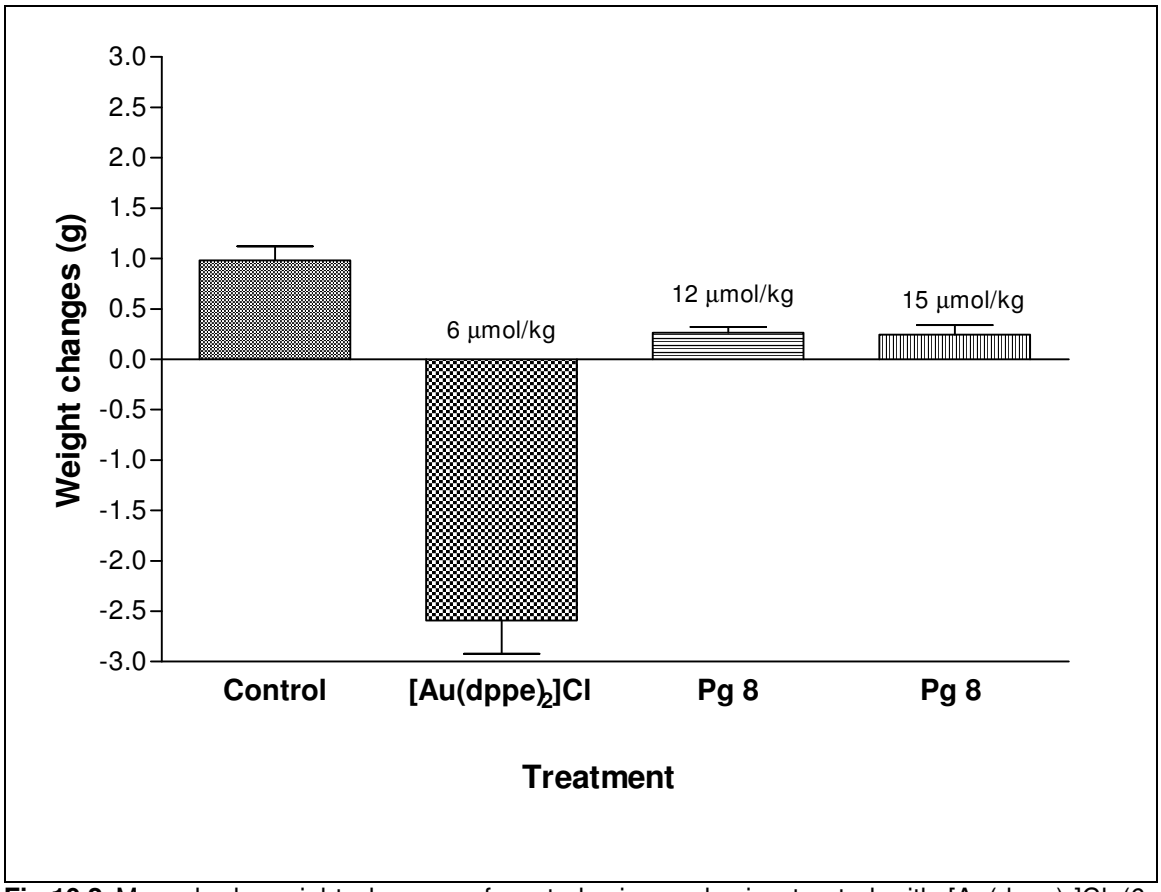

Fig.10.2 Mean body weight changes of control mice and mice treated with $[Au(dppe)_2]Cl$ (6 µmol/kg) and **Pg 8** (12 and 15 µmol/kg) in Phase 2 study.

In Phase 2, the mice in $[Au(dppe)_2]Cl$ (6 µmol/kg) group lost an average of 12.4% when injected with the compound for five days (*Fig 10.2*). The mice treated with **Pg 8** (12 and 15 µmol/kg) did not show a reduction in body weight but exhibited reduced weight gain. They gained an average of 1% of their total body weight which was less than that observed in the untreated mice (4.7 %).

After completion of Phase 2, the major organs were surgically removed and weighed. The results are tabulated below (*Table 10.3*).

Table 10.3: Mean organ weight and organ/body weight ratio of control mice and mice treated with $[Au(dppe)_2]Cl$ (6 µmol/kg) and **Pg 8** (12 and 15 µmol/kg) in Phase 2 study

Group	**Body weight (g)**	**Heart (g)**		**Liver (g)**		**Kidneys (g)**	
		g	%	g	%	g	%
Control	22.02	0.116	0.53	1.217	5.53	0.149	0.68
$[Au(dppe)_2]Cl$ (6 µmol/kg)	18.52	0.104	0.56	1.194	6.45	0.142	0.77
Pg 8 (12 µmol/kg)	22.38	0.120	0.54	1.321	5.90	0.153	0.68
Pg 8 (15 µmol/kg)	21.12	0.112	0.53	1.217	5.76	0.144	0.68

No significant gross pathologic differences were observed between the control and treated groups. The average heart and kidney weights did not differ significantly among all the groups but the mean liver weights of the mice exposed to $[Au(dppe)_2]Cl$ were greater (by ~1%) than the rest (*Table 10.3*). However, this could be as a result of reduced body weight.

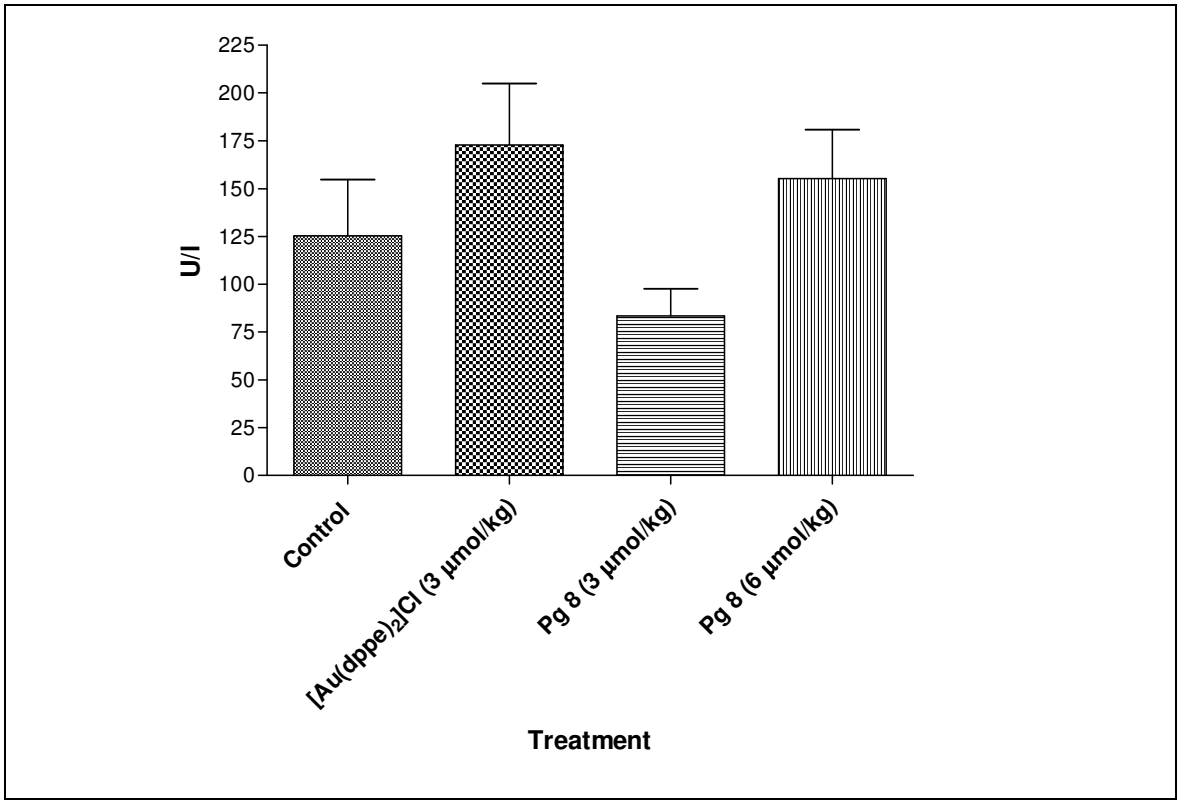

Fig. 10.3: AST levels of untreated mice and mice treated with $[Au(dppe)_2]Cl$ (3 µmol/kg) and **Pg 8** (3 and 6 µmol/kg) in Phase 1 study.

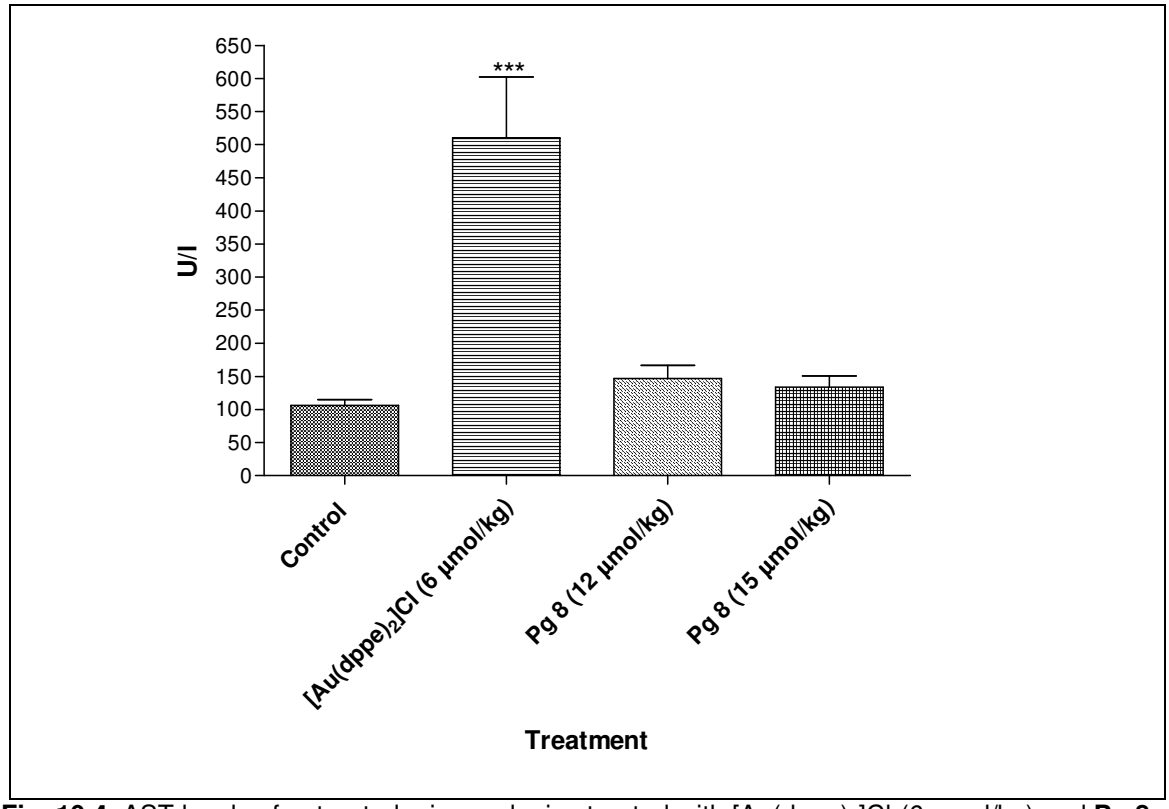

Fig. 10.4: AST levels of untreated mice and mice treated with $[Au(dppe)_2]Cl$ (6 µmol/kg) and **Pg 8** (12 and 15 µmol/kg) in Phase 2 study.

Analysis of liver enzyme AST, showed that there were no significant differences in their levels in all the groups (untreated and treated) in Phase 1 (*Fig. 10.3*). However, in Phase 2, the mice treated with $[Au(dppe)_2]Cl$ (6 µmol/kg) had significantly elevated levels of AST ($P<0.001$). These levels of AST were significantly higher than those found in the untreated and **Pg 8** (12 and 15 µmol/kg) treated mice (*Fig. 10.4*).

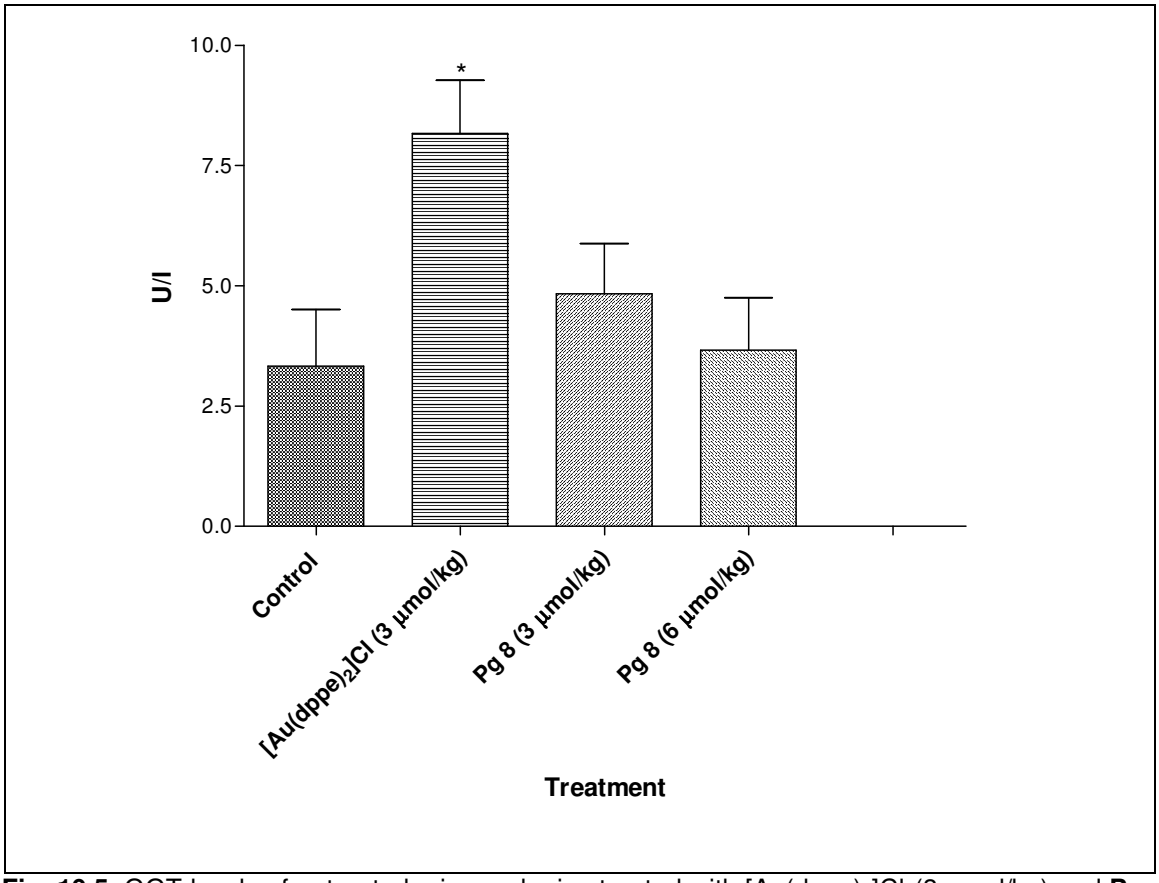

Fig. 10.5: GGT levels of untreated mice and mice treated with $[Au(dppe)_2]Cl$ (3 µmol/kg) and **Pg 8** (3 and 6 µmol/kg) in Phase 1 study.

GGT levels (*Fig.10.5*) were also slightly elevated (P <0.05) in the group treated with $[Au(dppe)_2]Cl$ (3 µmol/kg) when compared to the untreated mice. However, the levels did not differ significantly with the mice treated with **Pg 8** (12 and 15 µmol/kg)

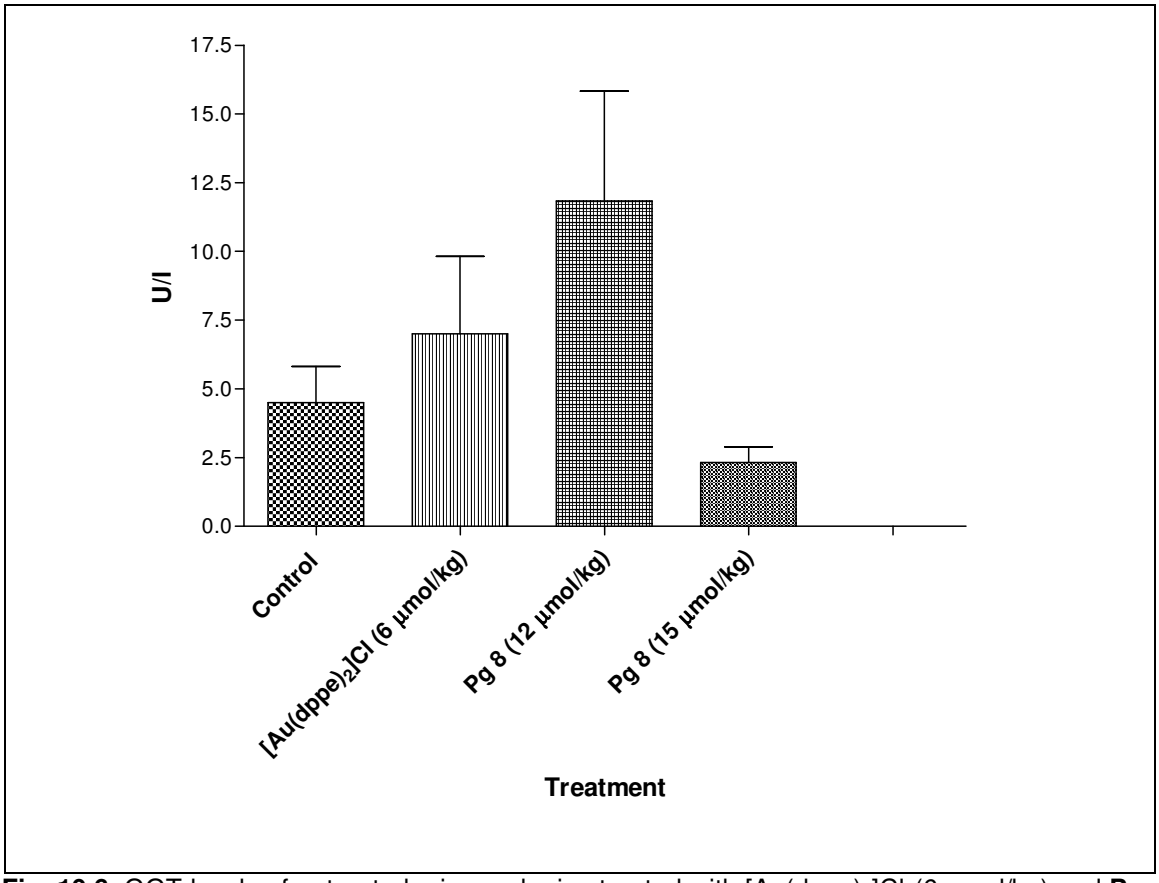

Fig. 10.6: GGT levels of untreated mice and mice treated with $[Au(dppe)_2]Cl$ (6 µmol/kg) and **Pg 8** (12 and 15 µmol/kg) in Phase 2 study.

In Phase 2 of the study, GGT levels did not show significant differences in all the groups (untreated and treated). Notably, the mice treated with 12 µmol/kg of **Pg 8** exhibited higher levels of GGT than the highest dose (15 µmol/kg). However, this difference was not significant.

Creatinine levels in all the groups did not vary (*Figs. 10.7 and 10.8*)[7]. This was an indication of lack of toxicity to the kidneys.

[7] Creatinine levels are expressed in mmol/l and not U/l as AST and GGT.

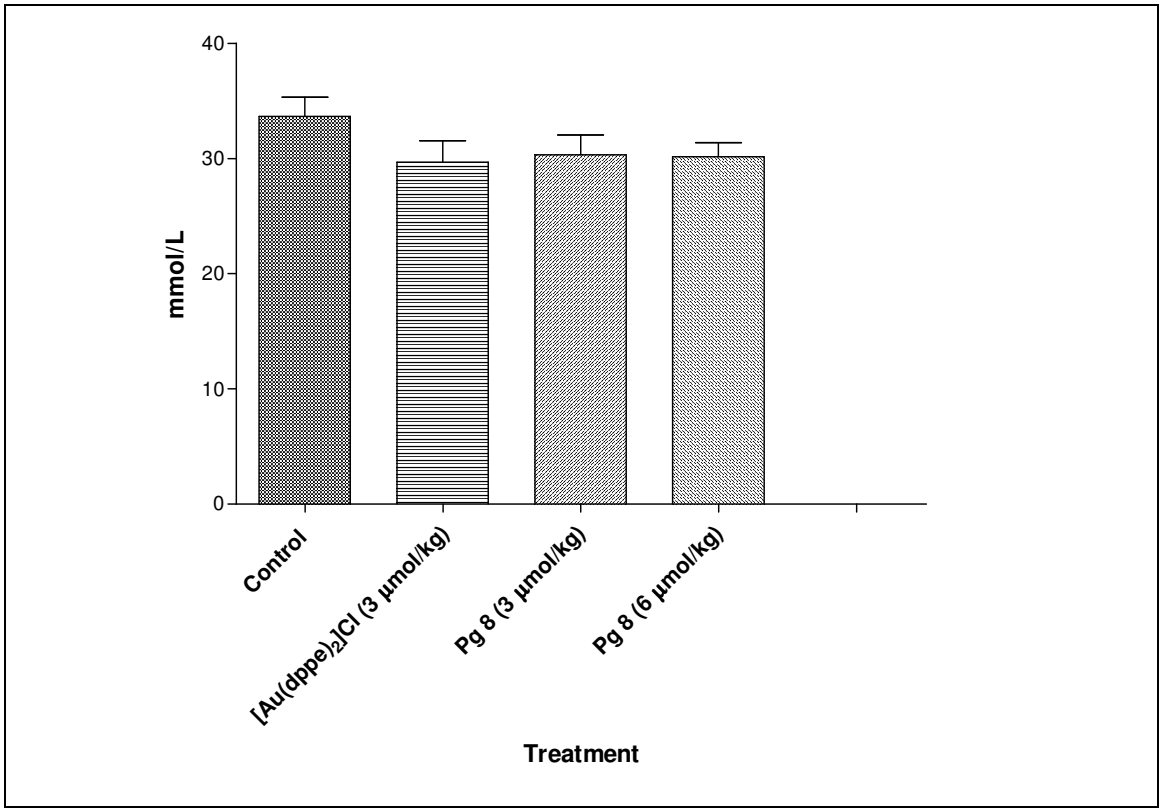

Fig. 10.7: Creatinine levels of untreated mice and mice treated with $[Au(dppe)_2]Cl$ (3 µmol/kg) and **Pg 8** (3 and 6 µmol/kg) in Phase 1 study.

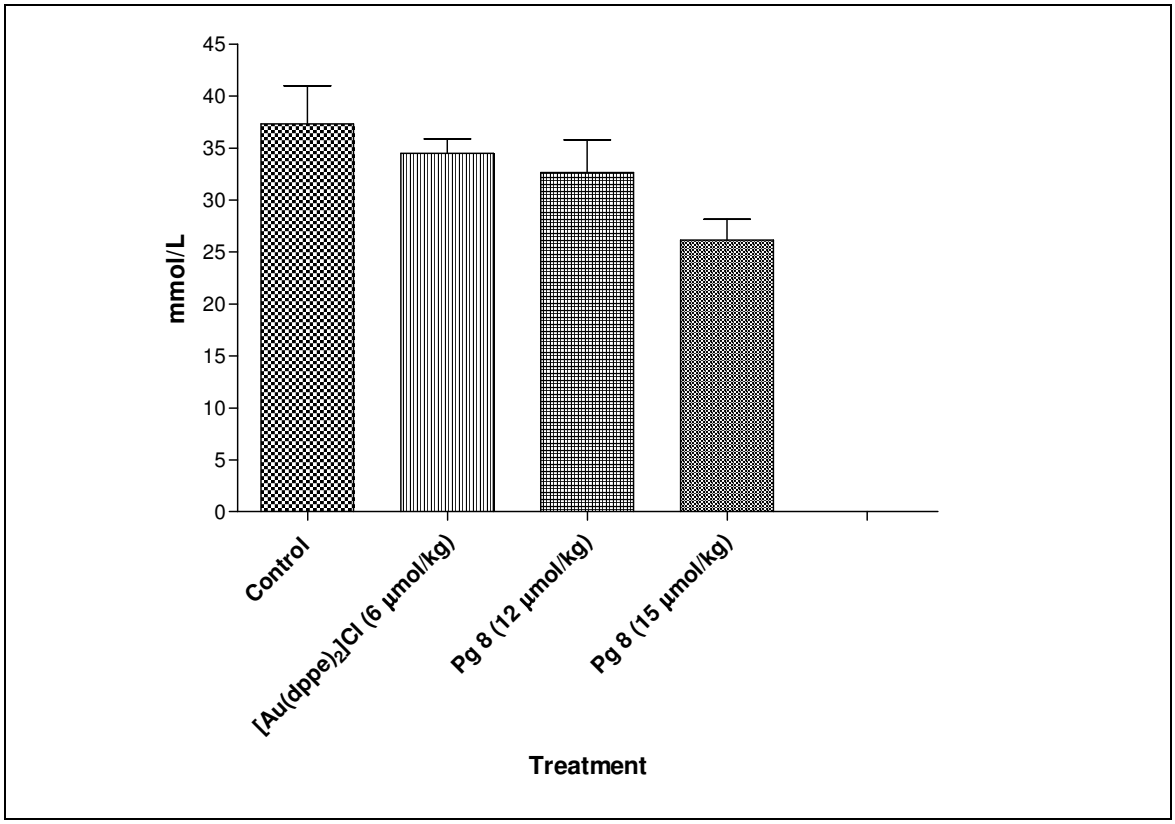

Fig. 10.8: Creatinine levels of untreated mice and mice treated with $[Au(dppe)_2]Cl$ (6 µmol/kg) and **Pg 8** (12 and 15 µmol/kg) in Phase 2 study.

No significant differences in full blood counts were observed as haematological parameters between the untreated and treated groups did not vary. Overall, the mice treated with $[Au(dppe)_2]Cl$ lost a greater amount of body weight than those treated with **Pg 8** at all concentrations. However, at higher concentrations (12 and 15 µmol/kg), the amount of weight gained over a period of 5 days was reduced in the latter compound. This observation was a sign that these elevated dosages caused discomfort to the animals. Subsequently, this could have led to reduced food intake. Analyses of the liver enzymes (AST and GGT) showed that $[Au(dppe)_2]Cl$ caused toxicity to the mice and this was contrary to the results obtained from the mice treated with **Pg 8**. Creatinine levels did not vary in all the experimental animals (untreated and treated).

Chapter XI

Conclusions

In the search for novel anti-cancer agents with mitochondrial mode of action, palladium and platinum derivatives of the known lipophilic cation $[Au(dppe)_2]Cl$ were prepared. This compound was shown to non-selectively target the mitochondria of all cells and research was stopped at pre-clinical phase due to severe host toxicity. To avoid similar problems, the ligand was varied in order to alter lipophilicity. Lipophilicity has been shown to play a role in determining toxicity as well as selectivity for cancer cells. The effect of changing the metal in analogous compounds was also investigated with special focus on reactivity, solubility, stability and biological activity. Cationic palladium and platinum phosphine complexes that were stable enough to undergo biological assays on cancer cells were synthesised.

Initially, dicationic complexes with Cl^- as a counterion were synthesised. The first compounds were complexed to 1,2-bis-(diphenylphosphino)ethane (dppe) and 1,2-bis-(diphenylphosphino)ethene (*cis*-dppen). The preparation of the 2, 3 and 4-pyridyl complexes proved more problematic than the phenyl ones. The reaction of the 1,2-bis-(di-2-pyridylphosphino)ethane with Pt or Pd led to production of both the *mono*-, $[MCl_2(d2pyrpe)]$ and *bis*-chelated, $[M(d2pyrpe)_2]Cl_2$ complexes irrespective of stoichiometry used. Separation of the mixtures by various methods proved futile as decomposition occurred.

This instability was attributed to the lability of the Cl and it was confirmed by stability tests carried out by ^{31}P NMR spectroscopy (**Chapter 5**). This necessitated a complete overhaul of the project as stability of a potential drug is of utmost importance if it is to retain its cytotoxic properties until it reaches the target (tumour cell). A pure product is also crucial as impurities would contribute to inaccurate results in biological studies. It was proposed that replacement of the counterion (Cl^-) with other counterions would be a suitable approach in ensuring stability. The first complex, $Pt(d2pyrpe)_2][BPh_4]_2$ proved to be stable and was successfully purified (as shown by X-ray crystallography). However, it precipitated out in the presence of cell culture medium and was non-toxic (IC_{50}> 50) to cervical cancer cells (HeLa). The other alternative, PF_6^- was proposed and the obtained compounds were purified without decomposition taking place.

The differences in reactivity between dppe and *cis*-dppen led to formulation of different synthetic routes. The final procedure for dppe complexes, $[Pt(dppe)_2][PF_6]_2$ and $[Pd(dppe)_2][PF_6]_2$, involved replacement of the chloride counter ion with PF_6 (crystal structure of latter compound was obtained). In the case of $[Pt(cis\text{-}dppen)_2][PF_6]_2$ and $[Pd(cis\text{-}dppen)_2][PF_6]_2$, chloride abstraction was in contrast carried out first before addition of the second dppen moiety. $[Pt(cis\text{-}dppen)_2][PF_6]_2$ was obtained in extremely low yields (19%) and this precluded its investigations in biological assays. Both dppe and *cis*-dppen metal complexes were extremely insoluble in various solvents and hence characterised mainly by ^{31}P NMR spectroscopy. The chemical shift differences between the *mono*- and *bis*-chelate compounds were used to monitor the reactions.

As mentioned earlier, preparation of the pyridyl complexes was very challenging. The preparation of the 2-pyridyl complexes for both metals was the simplest in this category. In the preparation of 3-pyridyl complexes, a 1:1 ratio (Na_2MCl_4:d3pyrpe) produced only *mono*-chelated complexes and addition of a second equivalent of ligand did not lead to the formation of the *bis*-chelated complexes. Substitution of the coordinated Cl in $[MCl_2(d3pyrpe)]$ with triflate was carried out but separation of the products was difficult. The mixtures were also insoluble in most solvents and hence identification was not possible by NMR spectroscopy. This route was also time consuming, laborious and led to great losses. It was not pursued further.

In the case of the palladium complexes, $[PdCl_2(NCMe)_2]$ was used instead of $Na_2[PdCl_4]$ but this gave more or less the same results. The synthesis of $[Pd(d3pyrpe)_2]Cl_2$ was quite problematic as the final product contained two phosphorus signals in ^{31}P NMR signifying the presence of two non-equivalent phosphorus atoms. Deduction of the structure was not possible from MS-FAB nor NMR but X-ray crystallography showed co-crystallisation of both *mono*- and *bis*-chelated chloride complexes, $[PdCl_2(d3pyrpe)]$ and $[Pd(d3pyrpe)_2]Cl_2$. While the preparation of $[Pd(d2pyrpe)_2][PF_6]_2$ (**Pg 8**) from a crude mixture of $[PdCl_2(d2pyrpe)]$ and $[Pd(d2pyrpe)_2]Cl_2$ led to a pure product (as shown by X-ray crystallography), similar attempts in metathesis failed in the case of the 3-pyridyl analogue. Similarly, the preparation of $[Pt(d3pyrpe)_2][PF_6]_2$ was distinctly different from the synthesis of the 2-pyridyl analogue.

Preparation of the 4-pyridyl complexes proved even more challenging than the 2 or 3-pyridyl ones. Decomposition products were obtained in most cases and in other cases, the reaction did not proceed to completion. Similar to [Pt(*cis*-dppen)$_2$][PF$_6$]$_2$ complex, the yield of the 4-pyridyl complex was so extremely low that satisfactory analyses could not be carried out. However, ^{31}P NMR studies showed that [Pt(d4pyrpe)$_2$]Cl$_2$ and [PdCl$_2$(d4pyrpe)] had been successfully obtained. In broad terms, identification of the intermediates and the final complexes was not straightforward by NMR spectroscopy. The ^{1}H NMR spectra were almost identical while the phosphorus chemical shift changes were very marginal in some cases. In general, the platinum complexes were obtained in lower yields than the palladium ones.

The trend observed in cytotoxicity assays carried out on cancerous cells indicated that palladium complexes were more toxic than the platinum ones. [Au(dppe)$_2$]Cl, which was the most lipophilic compound, exhibited the highest toxicity and non-selectivity. All the novel compounds were non-toxic to both resting and stimulated lymphocytes. From cytotoxicity assays (**Chapter 5**), one novel compound, **Pg 8** was selected as the lead compound as it exhibited the highest activity against a range of cancer cell lines. The hypothesis was that this toxicity was as a result of depolarisation of the mitochondrial membrane. Investigations to define its mode of action with special reference to the mitochondria led to various experiments. The mitochondria was selected as the target organelle because its analogue [Au(dppe)$_2$]Cl has been shown to act specifically on the mitochondria.

Analysis of mitochondrial membrane potential changes concluded that **Pg 8** did not depolarise the mitochondrial membrane of Jurkat cells even at high concentrations (10 and 15 µM) and neither after prolonged exposure (7 days). Similarly, this compound did not cause any changes in the plasma membrane potential when exposed to Jurkat cells for 24 h (10 and 15 µM). In contrast, exposure of **Pg 8** (0.711 and 1.422 µM) to Jurkat cells for 7 days showed that loss of plasma membrane potential began to take place from day 4. This observation seemed to be related to chemical changes that occurred as analysed by ^{31}P NMR spectroscopy.

In the quest to define the mode of action, induction of apoptosis by this compound was investigated. It was shown to induce apoptosis as well as necrosis to Jurkat cells after incubation for 48 h. Further investigations showed that **Pg 8** disrupted cell cycle progression of Jurkat cells after 48 h. There was a significant increase in number of cells in the S-phase signifying blockade in this phase. This disruption of cell cycle sequence may have led the cell to undergo apoptosis and necrosis followed by death. Studies with radiolabelled $[Au(dppe)_2]Cl$ and **Pg 8** on Jurkat cells showed that both complexes accumulated in the cells although the former compound accumulated in larger amounts. Biodistribution studies in Wistar rats showed that the gold compound seemed to accumulate in most organs, while most of the the palladium compound seemed to have been excreted.

This accumulation of the $[Au(dppe)_2]Cl$ in major organs may be the reason why it causes *in vivo* toxicity. Injection of the compound for 5 days caused Balb/c mice to lose a considerable amount of body weight at MTD (3 µM) and 6 µM. This sign of toxicity was expected as this compound was toxic to normal cells such as lymphocytes, chicken embryo fibroblasts and hepatocytes. In contrast, animals treated with **Pg 8** did not lose any body weight even at 15 µM. However, at this concentration, their weight gain was reduced when compared to the control group. Measurement of biochemical parameters revealed that AST, GGT and creatinine levels were not significantly elevated in mice treated with **Pg 8**. Groups treated with $[Au(dppe)_2]Cl$, showed marked elevation of AST and GGT levels.

The platinum complexes analysed in this study were less active on cancer cells than the palladium ones. This research has demonstrated that a balance between kinetic and thermodynamic properties of some palladium complexes may lead to development of compounds that show selective toxicity to cancer cells. This study has proven the hypothesis that varying the metal and lipophilicity may lead to modification of selectivity and cytotoxic properties of anti-neoplastic drugs containing Platinum Group Metals. In conclusion, **Pg 8** has the potential to be developed as an anti-cancer drug based on its role in cell cycle arrest and apoptosis as well as its lack of *in vivo* toxicity.